

Universidade de Lisboa

Faculdade de Farmácia



Evaluation of the immune response to SARS-CoV-2 in ICU patients with COVID-19

Carolina Santos Palma

Dissertation supervised by Professor João Gonçalves

Master in Biopharmaceutical Sciences

2021

Universidade de Lisboa

Faculdade de Farmácia



Evaluation of the immune response to SARS-CoV-2 in ICU patients with COVID-19

Carolina Santos Palma

Dissertation supervised by Professor João Gonçalves

Master in Biopharmaceutical Sciences

2021

**“SUCCESS IS GOING FROM FAILURE TO FAILURE
WITHOUT LOSING ENTHUSIASM...”
WINSTON CHURCHILL**

ACKNOWLEDGMENTS

First of all, I would like to thank my supervisor João Gonçalves for his unconditional support and guidance during this time of my life. Your enthusiasm and dedication to science is an inspiration to younger generations and an encouragement to continue pursuing my dreams in science. Thank you for accepting me in your lab team and for providing me with this unique opportunity.

Endless thanks to my dear colleagues,

Margarida Manuel who helped me settle into the lab and start my project.

Pedro Fontes, an amazing scientist, and a wonderful person. Thank you for all the encouragement and kind words.

A big, big thanks to my colleague Carlos Araújo, a very special person, for all the help with the experiments, for pushed me forward and constantly supported me, for the encouragement and kind words when I was losing my self and finally, for teaching me so many things during this time.

Also, an enormous thanks to my dear colleague Miguel Cardoso, who guided me during my initial project, who teach me so many things and who make me laugh during the hard times.

And to all the remaining lab members, for the debates in the lunch, for the bohemian conversations and for all the support, it was not possible without you.

A special thanks to my sisters from another mother Carina Tranquada, Joana Marçal and Margarida Rios Cruz for all the love, care, friendship, and good times. You will always have a very special place in my heart.

I would also like to thank my old friends Anna Goll and João Rocha for all the friendship and support during these years.

To my grandmothers, aunts, and uncles, and to my dear cousins Sara and Elias that always believe in my competencies. A special thanks for all the support.

And finally, an enormous thank you to my parents Olga and Jorge, to my brothers José and Afonso, and finally to my sister Cristina for their unconditional love and timeless support. Thank you for accompanying me during this journey, doing your best to be present in the good and bad times, for showing that with persistence, effort, and hard work all its possible.

ABBREVIATIONS

ARDS	Acute Respiratory Distress Syndrome
ACE2	Angiotensin Converting Enzyme 2
AUC	Area Under the Curve
BCR	B Cell Receptor
CCL	Chemokine
CD4/8	Cluster of differentiation 4/8
COVID-19	Coronavirus Disease 2019
CoV(s)	Coronavirus(es)
CRP	C-Reactive Protein
CP	Cut-off Point
CRS	Cytokine Release Syndrome
CTLA-4	Cytotoxic T Lymphocyte-Associated protein 4
CTLs	Cytotoxic T Lymphocytes
DAMPs	Damage-Associated Molecular Patterns
DFSO	Days From Symptom Onset
ECD	Ectodomain
ERGIC	Endoplasmic Reticulum-Golgi Intermediate Compartment
E	Envelope protein
ELISA	Enzyme-Linked Immunosorbent Assay
EDTA	Ethylenediamine Tetraacetic Acid
FDA	Food and Drug Administration
G-CSF	Granulocyte Colony Stimulating Factor
GM-CSF	Granulocyte Macrophage Colony Stimulating Factor
EC50	half maximal Effective Concentration
IC50	half maximal Inhibitory Concentration
TH	Helper T cells
HÁ	Hemagglutinin
HR	Heptad Repeats
HRP	Horseradish Peroxidase
HCoV(s)	Human Coronavirus(es)
Ig	Immunoglobulin
IP-10	Inducible Protein 10
ILCs	Innate Lymphoid Cell
ICU	Intensive Care Unit
IFN	Interferons
IL	Interleukin
MIP3a	Macrophage Inflammatory Protein 3
MHC	Major Histocompatibility Complex
M	Membrane protein
mRNA	messenger RNA
MERS	Middle Eastern Respiratory Syndrome

MCP	Monocyte Chemoattractant Protein
NK	Natural Killing
Nab(s)	Neutralizing Antibod-y (-ies)
NSP	Non Structural Proteins
N	Nucleocapsid protein
ORFs	Open Reading Frames
OD	Optical Density
PRRs	Pattern Recognition Receptors
PBS	Phosphate Buffer Saline
PD-1	Programmed cell Death protein 1
rRT-PCR	real-time Reverse Transcription Polymerase Chain Reaction
ROC	Receiver Operating Curve
RBD	Receptor Binding Domain
Tregs	regulatory T cells
RNA	Ribonucleic Acid
RdRp	RNA-dependent RNA polymerase
SARS-CoV-2	Severe Acute Respiratory Syndrome Coronavirus 2
S	Spike protein
sgRNA	sub-genomic RNA
TIGIT	T cell Immunoreceptor with Ig and ITIM domains
TCR	T cell Receptor
TMB	TetraMentylBenzidine
TGF	Transforming Growth Factor
TMPRSS2	Transmembrane Protease Serine Protease 2
TNF	Tumour Necrosis Factor

ABSTRACT

The coronavirus disease 2019 (COVID-19) pandemic, caused by the severe acute respiratory syndrome coronavirus 2 (SARS-CoV-2), has infected millions of people. Unprecedented efforts have been performed by the scientific community worldwide with the aim to develop an effective treatment or vaccine against SARS-CoV-2. The aim of this thesis was to characterize the immune responses triggered by SARS-CoV-2 in a cohort of severe COVID-19 patients. Analysis of antibody responses revealed that almost 100% of patients developed spike S1-, and nucleocapsid-specific IgM, IgG, and IgA antibodies, during intensive care hospitalization. On the other hand, Spike S2-specific IgG and IgM antibody responses were not detected. In addition, non-survival patients failed to develop high titers of antibodies against SARS-CoV-2 proteins tested. Moreover, in the early stage of hospitalization, patients already presented neutralizing antibody (NAb) titers yet relatively low. Median Nab titers increased during the first days of intensive care (IC) hospitalization and remained constant until discharge. Furthermore, characterization of antibody response to receptor-binding domain (RBD) epitopes from SARS-CoV-2 revealed the existence of two clusters of peptides, in which the reactivity of IC patients' plasma samples was higher. The immunoreactivity of cluster 2 stands out compared to cluster 1. This cluster is located in the RBD site of interaction with its receptor, the ACE2, suggesting that antibodies targeting these epitopes are more likely to be Nabs. Moreover, we showed that the COVID-19 signature was characterized by an upregulation of several pro-inflammatory cytokines and chemokines such as GM-CSF, TNF- α , IFN- γ , IL-1 β , IL-5, IL-6, IL-8, and MIP3a. Elevated cytokine levels were correlated with a worse disease prognosis. Non-survival patients revealed a divergent cytokine profile, characterized by either an exacerbated or a lack of response. We concluded that several mechanisms of host immune response are being implicated in COVID-19 immunopathogenesis. Antibody responses likely play an important role in COVID-19 progression and outcome. Furthermore, the cytokine signature responses may give important hints to clinicians and thereby raising the possibility to modulate the inflammatory immune response in the early disease stage avoiding bad clinical trajectories and ultimately death.

Keywords: COVID-19, SARS-CoV-2, ICU patients, immune response, antibodies, cytokines/chemokines

RESUMO

No final do ano de 2019, foi descoberto um novo vírus altamente contagioso ao qual se deu o nome de SARS-CoV-2, (*Severe Acute Respiratory Syndrome Coronavirus 2*) o qual provoca a doença COVID-19. Mundialmente, a disseminação contínua de COVID-19 tornou-se um enorme problema de saúde pública com consequências sociais, económicas e políticas devastadoras. Devido ao seu recente surgimento, existe uma grande carência de informação sobre o seu comportamento e da resposta imune do hospedeiro. Esta tese tem como objetivo caracterizar a resposta(s) imune(s) desencadeada pelo SARS-CoV-2 numa coorte de doentes internados nos cuidados intensivos (CI) com COVID-19. Além disso, também pretendemos encontrar padrões associados à qualidade e amplitude das respostas imunes nestes doentes. Os participantes do estudo foram recrutados no Hospital Curry Cabral, em Lisboa, de 14 de março a 14 de junho de 2020. Todos os participantes elegíveis tinham uma infeção provocada por SARS-CoV-2, confirmada por RT-PCR, e caracterizada por uma evolução clínica grave, o que resultou na sua admissão na unidade de cuidados intensivos (UCI) do hospital. De forma a acompanhar a progressão da doença ao longo do tempo de internamento, foram colhidas amostras de sangue aproximadamente a cada 3 dias em cada doente. Além disso, de acordo com os níveis de CRP monitorizados no momento de admissão nos cuidados intensivos, os doentes foram estratificados de acordo com o estado clínico em doentes graves (CRP<200µg/mL) ou doentes críticos (CRP>200µg/mL). Inicialmente, analisámos a resposta humoral mediada por anticorpos entre os dois grupos de doentes. Ao analisarmos os títulos de IgG e IgM específicos para a proteína spike S1, S2 e para a nucleocapside, não observamos diferenças significativas entre os 2 grupos, durante o tempo de permanência nos CI. No entanto, foi possível observar que os títulos de anticorpos IgM e IgG específicos para a spike S1 eram mais elevados quando comparados com os títulos para a nucleocapside. O que sugere que a proteína spike é mais imunogénica do que a nucleocapside, e que os anticorpos contra esta proteína têm um papel importante na eliminação viral e na recuperação dos doentes. Curiosamente, não detetamos níveis de anticorpos IgG e IgM específicos para a subunidade S2, mostrando a baixa imunogenicidade desta subunidade da proteína spike. Na admissão aos cuidados intensivos, os níveis de anticorpos IgG anti-spike S1 e anti-nucleocapsíde estavam 4 e 2 vezes aumentados, respetivamente, em relação ao *background* do ensaio de ELISA. No entanto, os títulos de anticorpos IgG continuaram a aumentar até aproximadamente ao 6º dia após a admissão, onde atingiram o *plateau*. Relativamente aos níveis de anticorpos IgM, estes permaneceram constantes durante o tempo de internamento no UCI. Os níveis de IgM específicos para a Spike S1 estavam 2 vezes aumentados relativamente ao cutpoint, enquanto os níveis de IgM específicos para a nucleocapsíde

estavam próximos do cutpoint. Relativamente, aos níveis de anticorpos IgA específicos para a S1 e para a N, observámos uma grande variação entre os dois grupos CRP-estratificados. Os títulos de anticorpos IgA aumentaram até atingir um pico por volta do 6º dia após a admissão na UCI, mas rapidamente decresceram até valores próximo do *background* do ensaio. Em contraste, a variação nas respostas de anticorpos foi extremamente díspar nos doentes críticos. Enquanto alguns doentes apresentavam uma resposta semelhante à observada nos doentes graves, outros não apresentavam qualquer resposta. Em suma, o perfil cinético da resposta dos anticorpos observado neste estudo é consistente com o reportado em estudos anteriores. No entanto, é possível observar variações temporais na cinética das respostas entre os vários estudos. É ainda importante notar que os doentes que sucumbiram ao COVID-19 não desenvolveram elevados títulos de anticorpos contra as várias proteínas SARS-CoV-2 testadas (Spike S1, S2 e Nucleocapsíde). Nos primeiros dias após entrada no UCI foi possível detetar títulos de anticorpos neutralizantes (NAb), porém esses títulos eram relativamente baixos. Destaca-se um aumento ligeiro nos títulos de NAb nos doentes graves em relação aos doentes em estado crítico. Em ambos os grupos, os títulos de NAb atingiram o seu pico aproximadamente ao 6º dia após a admissão na UCI, permanecendo estáveis durante o restante período de internamento. De forma geral, os doentes graves apresentaram uma resposta cinética para os anticorpos neutralizantes idêntica à dos doentes críticos, contudo apresentaram sempre níveis de NAb ligeiramente superiores. É, no entanto, de notar que os doentes que morreram não desenvolveram títulos de NAb ou o seu surgimento foi tardio, sugerindo que as respostas de anticorpos contra SARS-CoV-2 desempenham um papel essencial na sobrevivência à COVID-19. Foi ainda possível notar que os níveis de NAb estão fortemente correlacionados com os níveis de anticorpos IgG, mas não com as restantes classes IgM e IgA. Estudos anteriores demonstraram que os anticorpos neutralizantes direcionados para o domínio de ligação ao recetor (RBD) são imunodominantes durante as infeções por SARS-CoV-2. Com base nessas observações, decidimos estudar a reatividade das amostras de plasma dos doentes COVID-19 contra os epítomos do RBD do SARS-CoV-2. Observámos, pela primeira vez, a existência de dois *clusters* de peptídeos, *cluster 1* e *cluster 2*, nos quais a reatividade das amostras de plasma de doentes foi superior. Ao comparar a reatividade entre os dois *clusters* foi possível observar que o *cluster 2* apresentava reatividade superior em relação ao *cluster 1*. Curiosamente, ao analisar a localização dos *clusters* na estrutura tridimensional da proteína spike do SARS-CoV-2, vemos que o *cluster 2* está localizado no local de interação do RBD com o seu recetor, o ACE2 (*angiotensin-converting enzyme 2*), em contraste com o *cluster 1*, que está localizado no local oposto. Estas observações sugerem que os anticorpos direcionados a estes *clusters*, particularmente ao *cluster 2*, são mais prováveis de possuírem uma atividade neutralizantes. Ao analisar a resposta entre doentes graves e críticos não foi

possível encontrar diferenças significativas na imuno-reatividade dos peptídeos. No entanto, foi possível perceber que em ambos os grupos, alguns doentes exibiam um padrão distinto de reatividade para os diversos epítomos do RBD. Esses resultados sugerem que a progressão da doença não está inteiramente associada aos títulos e ao alvo dos anticorpos, mas também a outros mecanismos da resposta imune, como a resposta inflamatória mediada por citocinas. Foi ainda possível observar um aumento da reatividade ao longo do tempo de internamento em quase todos os doentes, sendo consistente com as melhorias observadas dos doentes. No entanto, mais estudos são necessários para confirmar a capacidade neutralizante dos anticorpos direcionados a esses dois *clusters*. Por último, mostrámos que a assinatura COVID-19 foi caracterizada por um aumento dos níveis de várias citocinas inflamatórias e quimiocinas, das quais destacamos as seguintes: GM-CSF, TNF- α , IFN- γ , IL-1 β , IL-5, IL-6, IL-8, e MIP3a. Os doentes que não sobreviveram, revelaram um perfil de citocinas divergente, caracterizado ou por uma resposta exacerbada ou pela falta de resposta. Os resultados apresentados neste trabalho demonstram que vários mecanismos da resposta imune do hospedeiro parecem estar implicados na imunopatogénese da COVID-19. Através da análise da resposta de anticorpos, podemos perceber que estes desempenham um papel importante na progressão e no desfecho clínico da COVID-19. Além disso, a análise da assinatura de citocinas pode dar orientações aos profissionais de saúde para modular a resposta imune inflamatória no estágio inicial da doença, evitando assim trajetórias clínicas graves e até a morte.

Palavras chave: COVID-19, SARS-CoV-2, doentes do UCI, resposta imunitária, anticorpos, citocinas/quimiocinas

TABLE OF CONTENTS

ACKNOWLEDGMENTS	6
ABBREVIATIONS.....	8
ABSTRACT	12
RESUMO	14
List of Figures.....	22
List of Tables.....	26
CHAPTER I: Introduction	28
1. CORONAVIRUS DISEASE 2019	32
1.1. Coronavirus Disease (COVID)-19: Emergence and spread.....	32
1.2. Classification and origin	32
1.3. SARS-CoV-2 genome and structure.....	34
1.4. Mechanism of infection	35
1.5. Clinical and epidemiological features	37
1.6. Diagnosis.....	38
1.7. Therapeutics drugs and Vaccines	38
2. IMMUNE RESPONSE TO SARS-COV-2.....	42
1.1. Immune system: an overview.....	42
1.2. Innate immune response to SARS-CoV-2.....	43
1.3. Adaptive immune response	45
1.3.1. T cell-based immunity	45
1.3.2. B cell based humoral immunity	46
3. THESIS AIM	50
CHAPTER II: Materials and Methods	52
1) Study design and human samples	54
2) Enzyme-linked immunosorbent assay (ELISA).....	54
a. Detection of IgG's and IgM's against SARS-CoV-2 by indirect ELISA.....	54
b. Screening of IgA antibodies against SARS-CoV-2	55
3) Cross-reactivity of antigens from nCoV-NL63 and the SARS-CoV	55
4) Surrogate virus neutralization assay	55
5) Epitope mapping.....	56
6) Cytokine and Chemokine Protein Quantification by Multiplex ELISA.....	57
7) Statistical analysis.....	57
CHAPTER III: Results	60

1. Characterization of Patients.....	62
2. Characterization of antibody responses to SARS-CoV-2	63
a. Longitudinal analysis of the antibody responses.....	66
b. Characterization of neutralizing antibody responses	68
3. Characterization of antibody response to RBD epitopes from SARS-CoV-2	71
4. Cytokine/chemokine immune responses.....	74
CHAPTER IV: Discussion and Future Perspectives	78
REFERENCES	88
ANNEXES.....	96

List of Figures

Figure 1| Schematic representation of SARS-CoV-2 genome. SARS-CoV-2 genome encodes 12 open reading frames (ORFs). ORFs 1a and 1b encode for the RNA polymerase and other non-structural proteins while the remaining ORFs encode for various structural and accessory proteins that help in assembly of the viral particle and evading immune response. (S-Spike; E-Envelope; M-Membrane; N-Nucleocapsid)..... 34

Figure adapted from: Perico et. al. " Immunity, endothelial injury and complement-induced coagulopathy in COVID-19, Nature Reviews.

Figure 2|SARS-CoV-2 structure. (A) Schematic representation of SARS-CoV-2 showing the different components of the viral particle. **(B)** SARS-CoV-2 viral particle under an electron microscope amplification. The virion surface is decorated with club-like projections constituted by the trimeric spike (S) creating a crown like appearance..... 35

Figure adapted from: <https://app.biorender.com/biorender-templates/figures/5e99f5395fd61e0028682c01/t-5f21e90283765600b08fbe9d-human-coronavirus-structure>

Figure 3| Replication cycle of SARS-CoV-2. Schematic diagram showing the general replication cycle of SARS-CoV-2. Infection starts with the attachment of Spike receptor binding domain (RBD) domain to angiotensin-converting enzyme 2 (ACE-2) receptor, which induces endocytosis (Step 1). Membrane fusion typically occurs in the endosomes resulting into nucleocapsid releasing to the cytoplasm (Step2). The genomic RNA (gRNA) serves as the template for translation of the RNA polymerase and other proteins necessary to virus assembly (Step3). Full-length gRNA is replicated via a negative-sense intermediate, and a nested set of sub-genomic RNA (sgRNA) species are synthesized by discontinuous transcription (Step 4 and 5). These sgRNAs encode viral structural and accessory proteins (Step 6). Particle assembly occurs in the ER-Golgi intermediate complex (ERGIC) (Step 7), and mature virions are released in smooth-walled vesicles via the secretory pathway (Step 8)..... 36

Figure from: <https://app.biorender.com/biorender-templates/figures/5e99f5395fd61e0028682c01/t-5e62669695014100889dfc54-coronavirus-replication-cycle-simplified>

Figure 4| COVID-19 patients stratification based on CRP blood levels. Patients with CRP above 200 µg/mL (orange) were classified as critical, while patients with CRP levels below or equal to 200 µg/mL (blue) were classified as severe. 62

Figure 5| Characterization of ELISA immunoassay performance. (A) Receiver-operating characteristic (ROC) analysis for evaluation of ELISA to detect reactivity to SARS-CoV 2 antigens and **(B)** cross-reactivity against other SARSs **(C)** Reactivity and **(D)** cross-reactivity of control and SARS-CoV-2 convalescent plasma to different antigens. Each dot represents a separate time point per subject (Healthy subjects, n = 50; COVID-19 patients, n = 17). Black lines indicate mean values. Statistical analyses were performed using an unpaired two-tailed Student's t-test. (se- sensitivity; sp- specificity; AUC- area under the curve) 65

Figure 6| Evaluation of the antibody responses to SARS-CoV-2 in IC- patients. (A) Comparison of different classes of antibodies between severe and critical COVID-19 patients at different time points after ICU admission. The boxplots show medians (middle line) and third and first quartiles (boxes), while the whiskers show the minimum and maximum values observed. Antibody levels were presented as the absorbance at 450 nm divided by the cut point (Abs/CP). Abs/CP ≥ 1 was defined as positive and Abs/CP < 1 as negative. **(B)** Scatter plots showing the correlations between CRP levels with all denoted antibody classes tested in critical and severe groups. Spearman's was used to evaluate the correlations. 67

Figure 7| Validation of in vitro neutralizing antibody assay to Sars-CoV-2. (A) Determination of sensitivity (Se), specificity (Sp), and cutpoint by ROC approach. Cutpoint (CP) was determined by comparing mean inhibition % of (Nab) sera samples from a control group composed by healthy age matched volunteers (N=15) and of COVID-19 patient sera samples (N=47). **(B)** Unpaired two-tailed student's t test was used between the two datasets, p-value < 0.05 . The inhibition (%) for each sample was calculated according to the following metric: $(1 - \text{sample optical density value} / \text{negative control optical density value}) \times 100$. AUC Area Under the Curve; *** Significance below $p < 0.0005$ 68

Figure 8| Assessment of Nab titers overtime and correlations with CRP, IgG, and IgA levels in COVID-19 ICU- patients (A), COVID-19 patients are represented by severe (blue dots) and critical (red dots) across three time points. Middle solid lines represent the median of Nab titer values and the upper and lower boxplot represent the 3rd and 1st quartiles while the whiskers show the maximum and minimum values. A student's t test was performed to determine the differences between datasets (severe vs critical). **(B)**, Correlations of Nab titers between CRP low and high levels (all data points were used) **(C)** with IgG levels and **(D)**, IgA divided by IgG levels. Spearman's rank test was used to performed correlations between variables. IC₅₀ - half maximal inhibitory concentration, EC₅₀ - half maximal effective concentration. * denotes p-value < 0.05 70

Figure 9| Schematic representation of the synthesized peptides covering the RBD domain. S1 subunit is shown in light blue and the RBD domain in dark blue, while S2 subunit is shown in orange. Each peptide is composed by 20 residues with an overlap of 10 amino acids between successive peptides. 71

Figure 10| SARS-CoV-2 RBD immunoreactivity in COVID-19 patients. The heatmap summarizes the immunoreactivity of SARS-CoV-2 RBD epitopes against IgG antibodies present in COVID-19 patients plasma samples, obtained at different times after ICU admission. Dark blue indicates low binding to the respective epitope while yellow to red indicates moderate to high binding. 72

Figure 11| Three-dimensional structure of Spike protein of SARS-CoV-2 and schematic representation of clusters 1 and 2. Surface and ribbon diagram of SARS-CoV-2 spike protein (A). Ribbon diagram of SARS-CoV-2 spike protein showing the interaction between RBD (blue) and its receptor, angiotensin-converting enzyme 2 (ACE2), represented in grey (B). The orange highlighted regions show the location of the most immunogenic peptides, which were grouped in cluster 1 (D) and

cluster 2 (C). Cluster 1 is composed of 6 peptides (Bio-NV-20, Bio-VN-20, Bio-YN-20, Bio-CY-20, Bio-SL-20, Bio-GF-20) while cluster 2 is composed of 4 peptides (Bio-NT-20, Bio-PV-20, Bio-NA-20, Bio-VV-20). Adapted from Protein Data Bank ID 7A94 and 7VXX. 73

Figure 12| Dysregulated cytokine responses in ICU COVID-19 patients. Heat map reveals a cytokine signature of immune responses associated to COVID-19 patients. Cytokine data were normalized according to variance measured on each individual cytokine dataset. Cytokine expression levels are represented by a color scale, ranging from intense red for the lowest to green for the highest expression levels. 75

Figure 13| Longitudinal analysis of altered cytokine levels between severe and critical COVID-19 patients. Left, comparison of cytokines levels between severe (green) and critical (orange) COVID-19 patients at different times after UCI admission. The boxplots show medians (middle line) and third and first quartiles (boxes), while the whiskers show the minimum and maximum observed, each dot represents a patient. Right, regression lines indicate cytokines progression along UCI stay time in severe (purple) and critical (orange) UCI patients. Shading represents 95% confidence interval (CI). P values were determined with unpaired, two-sided Mann–Whitney U-test. (ns $p > 0.05$; * $p \leq 0.05$; ** $p \leq 0.01$) 76

Extended Data Figure 1| Sequence of the spike protein. S1 domain is shown in blue and orange (RBD). S2 domain is shown in green. In underlined is shown the amino acid sequence used to generate the peptide library. 98

Extended Data Figure 2| Antibody responses against SARS-CoV-2. Specific IgG, IgM, and IgA against SARS-CoV-2 spike S1, nucleocapsid and spike S2 were measure in severe (a) and critical COVID-19 patients (b) at different times after ICU admission. Antibody levels were presented as the absorbance 450nm divided by the cut point. (absorbance/cut point - Abs/CP): S/CP > 1 was defined as positive and Abs/CP ≤ 1 as negative. 99

Extended Data Figure 3| Antibody responses against different SARS-CoV-2 antigens. Comparison of the different classes of antibodies between critical and severe COVID-19 patients at different time points after ICU admission. The boxplots show medians (middle line) and third and first quartiles (boxes), while the whiskers show the minimum and maximum observed. P values were determined with unpaired, two-sided Mann–Whitney U-test. No significative P values were obtained between the two groups. 100

Extended Data Figure 4| Association between CRP levels and clinical characteristics of the COVID-19 patients. (A) No significant difference in the CRP levels at the plateau was found between ≤ 60 y group (N = 10) and > 60 y group (N = 9) and (B) patients gender. Unpaired, two-sided Mann-Whitney U test was performed. (C) No association was found between the CRP levels at age, hospital stay and date from symptoms onset until ICU admission. Pearson correlation coefficients (r) and p value are depicted in plots. 100

Extended Data Figure 5| Longitudinal analysis of cytokine levels between severe and critical COVID-19 patients. Comparison of cytokines levels between severe (green) and critical (orange)

COVID-19 patients at different times after UCI admission. The boxplots show medians (middle line) and third and first quartiles (boxes), while the whiskers show the minimum and maximum observed, each dot represents a patient. P values were determined with unpaired, two-sided Mann–Whitney U-test. (ns $p > 0.05$; ** $p \leq 0.01$; * $p \leq 0.05$; *** $p \leq 0.001$; **** $p \leq 0.0001$)..... 101

List of Tables

Extended Data Table 1 | Cohort demographics and clinical characteristics. 102

Extended Data Table 2 | Amino acid sequence of the synthesized peptides and their location in the SPIKE sequence. 103

Extended Data Table 3 | Statistical analysis of cytokine levels among severe and critical groups and negative control. 104

CHAPTER I: Introduction

1. CORONAVIRUS DISEASE 2019

1.1. Coronavirus Disease (COVID)-19: Emergence and spread

Coronavirus disease 2019 (COVID-19) is an infectious disease caused by the newly discovered severe acute respiratory syndrome coronavirus 2 (SARS-CoV-2). The first cases of SARS-CoV-2 infection were reported in Wuhan, Hubei province, China, in December 2019. Its origin was epidemiologically linked to the local Huanan Seafood Wholesale Market that also traded live wild animals¹. Since then, SARS-CoV-2 has rapidly spread around the world and on 11 March 2020, the World Health Organization decided to declare COVID-19 a pandemic².

Daily reports of the increasing number of new cases continue to emerge from many countries. So far, SARS-CoV-2 has infected more than 52 million people across 213 countries and killed more than 1.2 million people (as of 14 November 2020)³.

Although many efforts have been done to stop the virus spread, these efforts have been hampered by a lack of knowledge. Understanding how and in what types of settings SARS-CoV-2 spreads is essential to create effective prevention measures in a way to break chains of transmission⁴. Moreover, generating knowledge on SARS-CoV-2 behaviour and host immune response is crucial for the development of more specific and effective therapies.

1.2. Classification and origin

Coronaviruses are a group of large (26 to 32 kb) enveloped viruses with non-segmented, single-stranded, positive-sense ribonucleic acid (RNA) genomes. They are known to infect humans and animals, causing respiratory and sometimes gastrointestinal diseases⁵.

According to the International Committee on Taxonomy of Viruses, coronaviruses (CoVs) are categorized under the order *Nidovirales*, family *Coronaviridae*, and subfamily *Coronavirinae*. The *Coronavirinae* subfamily is subdivided into four genera: *Alphacoronavirus* which includes the human coronaviruses (HCoVs)-229E and HCoV-NL63; *Betacoronavirus* which integrates HCoV-OC43, HCoV-HKU1, Severe Acute Respiratory Syndrome (SARS)-CoV and Middle Eastern Respiratory Syndrome (MERS)-CoV; *Gammacoronavirus*, and *Deltacoronavirus* which comprise viruses isolated from mammals and birds⁵.

SARS-CoV-2 belongs to the Betacoronavirus genus, and much like the HCoVs, SARS-CoV and MERS-CoV, which have caused two large-scale epidemics in 2002 and 2012,

respectively, it also can replicate in the lower respiratory tract and cause severe respiratory problems which can be fatal⁶.

Since the first reports of SARS-CoV-2 infection, there has been considerable discussion on its origin. Epidemiological studies have suggested that the outbreak was associated with the seafood market of Wuhan. However, its role in the propagation of the disease is still unclear⁶.

The phylogenetic analysis of the SARS-CoV-2 genome revealed that it shares 79.6% sequence identity with the previous SARS-CoV and 50% with MERS-CoV⁷. In addition, a high similarity was obtained when compared SARS-CoV-2 to bat SARS-CoV-like coronaviruses. The closest relative to SARS-CoV-2, known to date, is a bat coronavirus discovered in Yunnan, named 'RaTG13'. It exhibits 96.2% identity to SARS-CoV-2. Another related bat coronavirus, named 'RmYN02', has been detected more recently, and although it shares a lower sequence identity with SARS-CoV-2 (93.3%) when compared to 'RaTG13', it exhibits a 97.2% identity to SARS-CoV-2 in the ORF1ab (see next section), which is even higher than for RaTG13. Besides RaTG13 and RmYN02 viruses, the phylogenetic analysis also reveals two bat coronaviruses, ZC45 and ZXC21, that fall into the SARS-CoV-2 lineage. The discovery of these diverse bat coronaviruses related to SARS-CoV-2 highly suggests that SARS-CoV-2 may have originated from bats. Nevertheless, these bat coronaviruses cannot be direct progenitors of SARS-CoV-2 as the divergence between them and SARS-CoV-2 likely represents several years of sequence evolution. Thus, these bat coronaviruses can only be regarded as the likely evolutionary precursors of SARS-CoV-2⁶⁻¹⁰.

Beyond bat coronaviruses, similar coronaviruses were found with up to 92.4% sequence homology to SARS-CoV-2 in the Malayan pangolins illegally imported into Guangdong province, where they are used illegally for medical purposes. Notably, the receptor binding domain (RBD) of the Guangdong pangolin coronaviruses is one of the most similar to that of SARS-CoV-2. The discovery of pangolin coronaviruses related to SARS-CoV-2 led some authors to suggest that these animals are possible intermediate hosts in the SARS-CoV-2 transmission route to humans. An intermediate host usually plays an important role in the outbreak, as was demonstrated by palm civets in the SARS-CoV outbreak and by dromedary camels in the MERS-CoV outbreak. The virus strains carried by these two intermediate hosts were more than 99% identical to the corresponding human virus. Thus, currently, there is no sufficient data to support pangolins as the intermediate host of SARS-CoV-2 despite the RBD resemblance to that of SARS-CoV-2^{11,12}.

Although bats are the most likely reservoir hosts, the animal origin of SARS-CoV-2 remains unknown. Likewise, it remains to be determined whether SARS-CoV-2 has been transmitted to man via an intermediate host and which animals can act as its intermediate host.

1.3. SARS-CoV-2 genome and structure

SARS-CoV-2 genome holds all the information needed to produce new virions after the infection. The genome comprises 12 open reading frames (ORFs). At the 5' end of SARS-CoV-2 genome are located two overlap ORFs (ORFs 1a and 1b) that encode for the RNA polymerase and other non-structural proteins. Downstream from ORFs 1ab, lies the remaining genes that encode for the structural and non-structural viral proteins involved in viral assembly and also in evasion of host immune response^{5,13}.

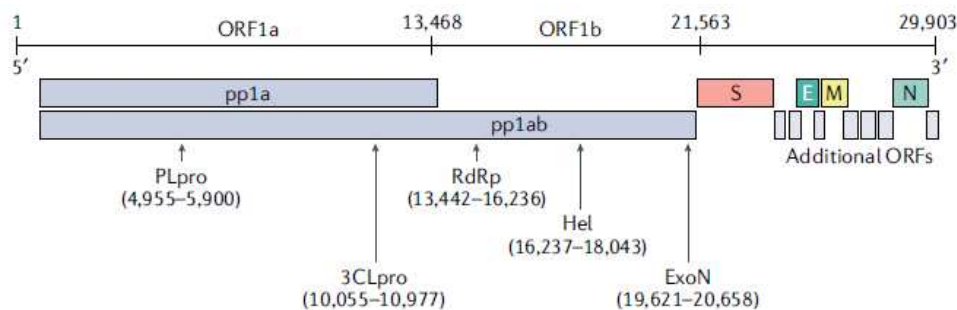


Figure 1 | Schematic representation of SARS-CoV-2 genome. SARS-CoV-2 genome encodes 12 open reading frames (ORFs). ORFs 1a and 1b encode for the RNA polymerase and other non-structural proteins while the remaining ORFs encode for various structural and accessory proteins that help in assembly of the viral particle and evading immune response. (S-Spike; E-Envelope; M-Membrane; N-Nucleocapsid).

SARS-CoV-2 genome is packed inside a helical capsid formed by the nucleocapsid protein (N), which is further surrounded by an envelope. The nucleocapsid protein is highly phosphorylated, resulting in its high affinity for viral RNA. Furthermore, the N protein plays critical roles in viral replication cycle and modulation of host immune response^{14,15}.

Associated with the viral envelope are three main structural proteins: the envelope (E), the membrane (M), and the spike (S) proteins, which are incorporated in the lipid bilayer. The M protein is the most abundant protein and is responsible for the support of the viral envelope. It also defines the viral structure and helps in the binding to the nucleocapsid which helps in its stabilization. The E protein is the smallest protein in the SARS-CoV-2 structure, and its role is associated with the production and maturation of the virus, and also with the virus assembly and egress. The last component is the S protein, which is expressed on the surface of the virus particles creating a crown effect when observed by electron microscopy (hence the name

corona, which derived from Latin and means crown). The S protein is a trimeric glycoprotein that mediates the virus entry into the host cells. This glycoprotein comprises two subunits known as S1 and S2. The S1 subunit consists of a receptor binding domain (RBD) while the S2 domain consists of a fusion peptide region and two heptad regions (HR1 and HR2). These subunits are responsible for the binding and membrane fusion to the host cell, respectively¹⁴.

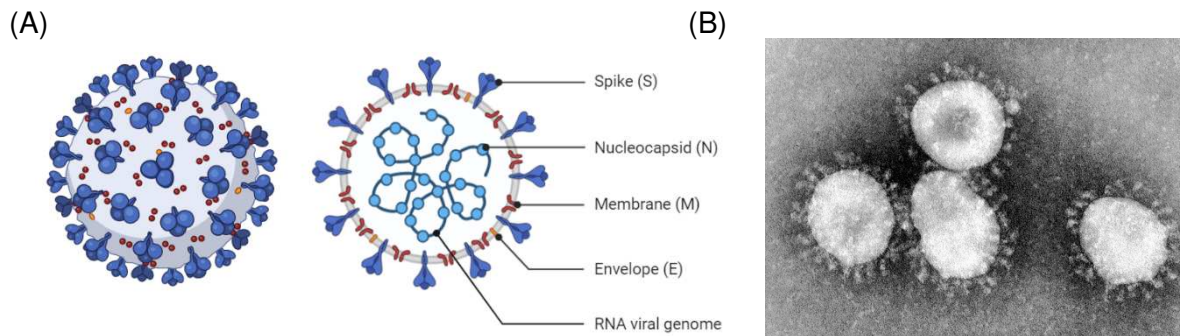


Figure 2|SARS-CoV-2 structure. (A) Schematic representation of SARS-CoV-2 showing the different components of the viral particle. **(B)** SARS-CoV-2 viral particle under an electron microscope amplification. The virion surface is decorated with club-like projections constituted by the trimeric spike (S) creating a crown like appearance.

1.4. Mechanism of infection

SARS-CoV-2 replication cycle begins when the binding domain of S protein (RBD) recognizes and binds to the receptor angiotensin-converting enzyme 2 (ACE2) present in the membrane of the airway epithelial cells, alveolar epithelial cells, vascular endothelial cells, macrophages, among others cells^{1,13,14}. Recent studies have demonstrated that cellular heparin sulfate has an important role in Spike-ACE2 interaction. The binding of SARS-CoV-2 to cellular heparin sulfate promotes the conformational change of the RBD, which results in an increase in its affinity for the ACE-2 receptor¹⁶.

Similarly to previous coronaviruses, SARS-CoV-2 requires the proteolytic processing of the S protein to activate the endocytic route. It has been demonstrated that several host proteases are involved in the cleavage of the S1 subunit and activation of SARS-CoV-2 entry, including transmembrane protease serine protease 2 (TMPRSS2), cathepsin L, and furin. Inside the endosome, the fusion peptide present in the S2 subunit, exposed by the proteolytic cleavage, is inserted in the host membrane. This step allows the S2 region to fold in on itself to bring the two heptad repeats (HR1 and HR2) together, which leads to membrane fusion and the nucleocapsid release into the host cell cytoplasm^{1,13,14,17,18}.

Once inside the cell, the viral genome starts its translation. The ORF-1a and ORF-1b are the firsts to be translated, resulting in the production of two large polyproteins pp1a and pp1b. These proteins are then cleavage by three proteases originating 16 non-structural proteins (NSP1-16), which will generate the viral RNA polymerase and other proteins necessary to virus assembly^{1,13,14}.

Full-length gRNA is replicated via a negative-sense intermediate, and a nested set of sub-genomic RNA (sgRNA) species are synthesized by discontinuous transcription into numeral structural and accessory proteins. The viral envelope proteins (S, M, and E) produced are incorporated in the rough endoplasmic reticulum or in the Golgi membrane, while the newly transcribed genome is combined with the N protein, in the cytoplasm, to form the viral nucleocapsid. The assembly of the viral particles occur in the Endoplasmic reticulum-Golgi Intermediate Compartment (ERGIC)^{1,13,14}.

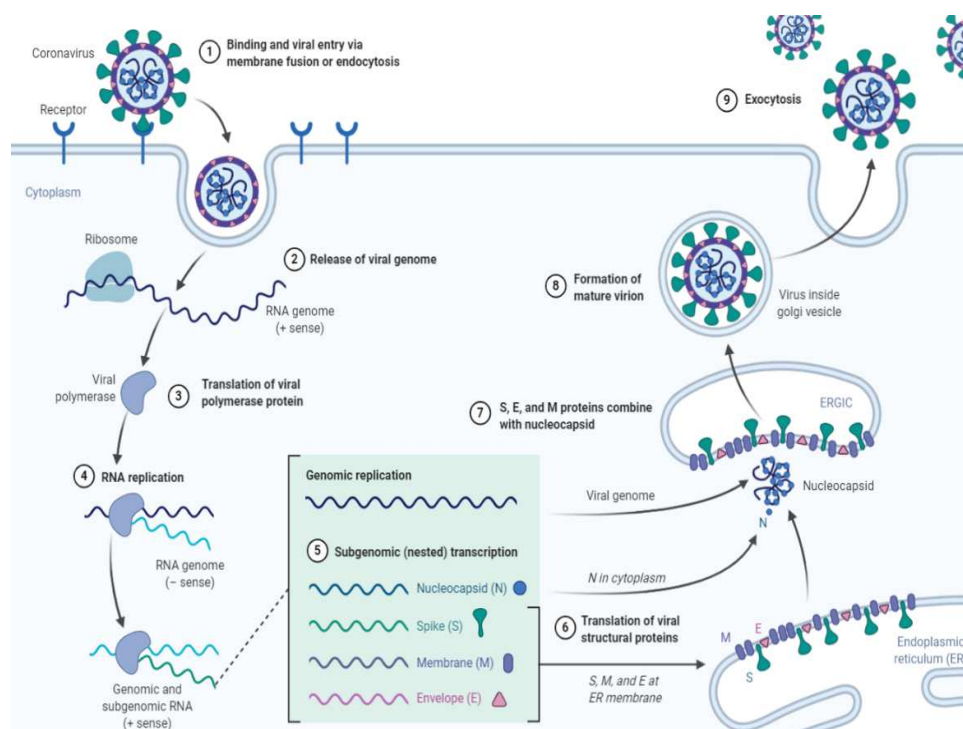


Figure 3| Replication cycle of SARS-CoV-2. Schematic diagram showing the general replication cycle of SARS-CoV-2. Infection starts with the attachment of Spike receptor binding domain (RBD) domain to angiotensin-converting enzyme 2 (ACE-2) receptor, which induces endocytosis (Step 1). Membrane fusion typically occurs in the endosomes resulting into nucleocapsid releasing to the cytoplasm (Step2). The genomic RNA (gRNA) serves as the template for translation of the RNA polymerase and other proteins necessary to virus assembly (Step3). Full-length gRNA is replicated via a negative-sense intermediate, and a nested set of sub-genomic RNA (sgRNA) species are synthesized by discontinuous transcription (Step 4 and 5). These sgRNAs encode viral structural and accessory proteins (Step 6). Particle assembly occurs in the ER-Golgi intermediate complex (ERGIC) (Step 7), and mature virions are released in smooth-walled vesicles via the secretory pathway (Step 8).

Lastly, the virus particle-loaded vesicles are fused with the cell membrane for effective shedding of the virus. These new virions are now mature and capable of infecting the neighbouring healthy cells^{1,13,14}.

1.5. Clinical and epidemiological features

SARS-CoV-2 clinical manifestations are characterized by a large range of symptoms. The most common symptoms of COVID-19 illness are fever, dry cough, dyspnoea, fatigue, and myalgia. Many infections, particularly in young people and children are asymptomatic (without symptoms). On the contrary, older people (≥ 60 years old), and those with underlying medical problems (comorbidities) like cardiovascular disease, diabetes, renal insufficiency, obesity, chronic respiratory diseases, and other diseases that compromise the immune system, are more likely to progress to a severe respiratory disease denominated acute respiratory distress syndrome (ARDS)^{1,19}.

ARDS observed in COVID-19 patients is characterized by difficulty in breathing and low oxygen levels. As a result, some patients may evolve directly to respiratory failure, which is responsible for 70% of COVID-19 fatalities. On the other hand, advanced stages of ARDS can evolve to septic shock since patients become more susceptible to fungal and bacterial infections. The excessive release of pro-inflammatory cytokines by the innate immune system (cytokine storm) in response to the viral and the secondary infections leads to uncontrolled inflammation, which may affect various organ systems, mainly the cardiac, hepatic, and renal. Most patients who progressed to multi-organ failure eventually died, representing 28% of fatal COVID-19 cases^{1,20,21}.

Like the other respiratory coronaviruses, COVID-19 virus spreads primarily through respiratory droplets produced when an infected person coughs, sneezes, or speaks. The transmission may also occur indirectly through contact with contaminated surfaces and objects (fomites)^{4,19,1}. SARS-CoV-2 viruses can be found in fomites for periods ranging from hours to weeks, depending on the type of surface and environment. Further, some scientists also refer to a possible faecal-oral transmission route, but remains unproven^{22,23}. These findings explain the rapid spread of SARS-CoV-2 infections among the population. Public health interventions to minimise the transmission among the population are being applied by the different governments in order to mitigate the pandemic. These interventions have proved successful in several countries including in China and South Korea where the cases per day are currently very low¹².

1.6. Diagnosis

Early detection of SARS-CoV-2 infection is crucial for controlling the spread of COVID-19 disease. The decision to test individuals against SARS-CoV-2 infection should be based on clinical and epidemiological factors. Consequently, patients with symptoms correlated with the COVID-19 disease, as well as a history of contact with other infected patients, should undergo a diagnostic test as soon as possible. SARS-CoV-2 infection can be confirmed through the detection of unique molecular signatures by nucleic acid amplification techniques, such as the real-time Reverse Transcription Polymerase Chain Reaction (rRT-PCR). Many of these amplification techniques commercially available target the ORF1b (including RNA-dependent RNA polymerase (RdRp)), N, E, or S genes²⁴. The virus normally can be detectable in the upper respiratory tract in the early stages of infection through throat swabs, posterior oropharyngeal saliva, and nasopharyngeal swabs, and in the lower respiratory tract, normally in sputum and bronchial fluid obtained by endotracheal aspirate or bronchoalveolar lavage²⁵. However, the lower respiratory samples are only required if the initial upper respiratory samples are negative but remain a strong clinical suspicion of COVID-19²⁶. Besides, SARS-CoV-2 can be detected in a broad range of other body fluids, including samples from the intestinal tract and blood^{27,28}. Other detection methods are used to obtain a rapid result, this includes tests that detect the presence of SARS-CoV-2 antigens in respiratory tract specimens without requiring the amplification of the target. Nevertheless, this makes the test less sensitive and more susceptible to false negatives²⁴. Besides nucleic acid tests and antigen tests, antibody tests, also known as serological tests, can be used to detect SARS-CoV-2 infections in an indirect way. Serological tests detect antibodies produced during the human immune response to SARS-CoV-2 infections²⁹. However, this type of test should not be used as a stand-alone diagnosis to identify SARS-CoV-2 infections, as the test does not detect the presence of the SARS-CoV-2, and therefore the tests can show negative results even in infected patients, for example, if the patients have not yet developed antibodies in response to the virus. The great utility of this test resides in the capacity to support the retrospective assessment of the infection rate and the size of the outbreak since it has the capacity to detect patients with past SARS-CoV-2 infections, including asymptomatic infections²⁴.

1.7. Therapeutics drugs and Vaccines

To date, there is no worldwide approved vaccines or specific therapeutics to prevent or treat COVID-19, although some therapies have shown some benefits in certain subpopulations of patients. Large-scale clinical trials to evaluate various therapies for COVID-19 are being conducted around the world by several research groups and manufacturers. Three different

approaches are being used to target SARS-CoV-2 infections: repurposing drugs, which consist in the re-purposing of an approved drug originally developed for the treatment of a different disease or medical condition; new therapeutic drugs, and vaccines.

As of 14 November 2020, there were about 437 therapeutic drugs in development for COVID-19, of which 350 were in human clinical trials. Some of those therapies are best suited to help during a certain stage of infection, while others target the host inflammation response. At the moment, just three therapeutic drugs have been approved to treat COVID-19 including dexamethasone in the United Kingdom and Japan; Favilavir in China, Italy, and Russia; and Remdesivir in the United States, Japan, and Australia. All these three drugs are repurposed drugs. Dexamethasone is a type of corticosteroid medication and a potent anti-inflammatory compound used to treat many conditions, including inflammatory and autoimmune conditions. This drug has been repurposed to COVID-19 treatment and the preliminary results demonstrated that a low dose of dexamethasone can reduce mortality in approximately one-third in COVID-19 patients on invasive ventilators and by one-fifth of patients on oxygen therapy. Favilavir and Remdesivir are two viral replication inhibitors that target the RdRp. A clinical study reported that Remdesivir can shorten the recovery time in hospitalized adults with COVID-19 by a couple days compared with placebo. However, it appeared to have no impact in mortality, initiation of ventilation and duration of hospital stay. Similarly, Favilavir reduce the time for viral clearance. Convalescent plasma treatment is another adjuvant therapy for COVID-19. Preliminary results have suggested improved clinical status after the treatment, however more data are required. On 23 August 2020, convalescent plasma treatment has received the Emergency Use Authorization by the FDA for treatment of patients with COVID-19. Furthermore, monoclonal neutralizing antibodies are another potential therapy for COVID-19. Several antibody therapeutics are now in phase II and III trials with promising results (e.g REGN-CoV-2, CT-59 and LyCoV555) ³⁰.

In contrast to the therapeutic drugs, which help to combat the disease, vaccines prevent the establishment of the disease, making it the most effective method for a long-term strategy for the prevention and control of COVID-19. Currently, there are about 179 vaccines in development, and nearly 52 in human clinical trials (as of 14 November 2020). Several of these vaccine candidates are in phase II testing, and some have already advanced to phase III trials with promising results. Many different strategies have been employed to develop these vaccines, including the use of recombinant vectors, DNA, mRNA coated in lipid nanoparticles, inactivated viruses, live attenuated viruses, and protein subunits. The vaccine AZD1222 (formerly ChAdOx1 nCoV-19) developed by the University of Oxford and licensed to AstraZeneca, was developed based on attenuated adenovirus that displays the SARS-CoV-2

spike protein on its surface. Initial phases I, and II, demonstrated that patients elicited both a humoral and cellular immune response upon vaccination. Although the phase III study was put on hold due to serious adverse reactions in two participants, the United States of America Food and Drug Administration (FDA) recently authorized the restart of phase III trials. Another vectored vaccine, Ad5-nCov, was developed by CanSino Biologic on the basis of adenovirus type 5-vectors which express SARS- CoV-2 S protein. The vaccine has proved to be safe and capable of inducing considerable immune responses in most recipients after a single immunization. This vaccine is currently approved for military use in China. Regarding inactive viral vaccines, BBIBP-CorV vaccine was developed by Sinopharm and was found to be safe and capable of generating strong antibody responses against numeral viral antigens during phases I and II clinical trials. Sinovac also developed an inactive viral vaccine, known as Coronovac. Coronovac exhibits a safety profile in both young and older participants. However, the elicited immune responses were slightly weaker on older participants according to preliminary results. The biotechnology company Moderna in conjunction with the National Institute of Allergy and Infectious Diseases (NIAID), develops mRNA-1273, a lipid nanoparticle containing the mRNA that encodes the stabilized prefusion SARS- CoV-2 S protein. The results of phase I clinical trial have revealed robust humoral and cellular immune responses in vaccinated individuals. The candidate mRNA vaccine from BioNTech Pharmaceuticals and Pfizer, BNT162, recently released the first results from its 45,538-person trial in a press release. The initial results shown that the vaccine is highly effective in preventing COVID-19, with an efficacy superior to 90%, but the trial is still going on and more data about the safety of the vaccine are needed³⁰.

2. IMMUNE RESPONSE TO SARS-COV-2

2.1. Immune system: an overview

Understanding how the human immune system works is extremely important for making sense of all the information around the risk and treatment of diseases like COVID-19. The human immune system is a complex network of organs, cells, and molecules that can detect and defend the body against harmful organisms through a variety of mechanisms. These harmful organisms are designated pathogens and are generally bacteria, viruses, fungi, or parasites. To function properly the human immune system must have the capacity to distinguish these pathogenic agents from itself, and it must work in a controlled manner in order to avoid severe damage of the human body^{31,32}.

The immune system can be divided into different systems, the innate immune system, and the adaptative immune system. The innate immune system, also called native immune system, forms the first line of defence against invading pathogens. It consists in cellular and biochemical defence mechanisms that are always ready to react to threats. These mechanisms are general and broadly specific, reacting always in the same way independently of the threat. The principal components of the innate immune response are physical and chemical barriers, such as the mucosal epithelia and the antimicrobial molecules produce by the epithelial cells; a variety of cells, including phagocytic, dendritic, and natural killing (NK) cells; and molecules which includes the members of the complement system and other mediators of inflammation like cytokines³¹⁻³³.

Contrasting with the innate system, the adaptative immune system is far more powerful and specific. It is characterized by its specificity for different pathogens and by its ability to remember (immunological memory). The adaptative system can be divided in two types of responses, the humoral response and the cell-mediated response which are mediated by different components of the immune system. Humoral immunity is mediated by B lymphocytes and their secreted products, antibodies, and functions in defence against extracellular pathogens. Cell-mediated immunity is based in T lymphocytes responses and is crucial for defence against intracellular pathogens³¹⁻³³.

Both systems have an essential role in recognizing and eliminating pathogens. However, a suboptimal or uncontrolled immune response during SARS-CoV-2 infection drives to increased disease severity and worse COVID-19 prognosis. Identification of specific immune signatures may provide a better comprehension of the different disease trajectories.

2.2. Innate immune response to SARS-CoV-2

The innate immune system aims to block the entry of viruses and eliminate or limit their growth before they colonize the host tissues³². To date, our understanding of the specific innate immune response to SARS-CoV-2 is extremely limited. However, given the high similarity of SARS-CoV-2 with the previous coronaviruses and the conserved mechanisms of the innate immune response, it is likely that SARS-CoV-2 virus-host interactions resemble those previously described³⁴.

The physical barriers located in the sites of interaction between the host and the environment are the first obstacles to the viral infection. If the virus successfully breaches these barriers, it will face the innate immune cells present in the tissues. The cellular innate immune response to pathogens like SARS-CoV-2 can be divided in two main types of reactions: inflammation and antiviral defence. Inflammation is the process by which leukocytes and plasma proteins are recruited to the site of infection, where they will be activated to destroy the viral particles. In contrast, the antiviral defence consists of a cytokine-mediated reaction, normally interferons, in which cells acquire resistance to viral infection; and increasing the susceptibility of leukocytes to kill virus-infected cells³².

The innate immune cells detect viral infections by using a variety of cellular receptors, often called, pattern recognition receptors (PRRs), which recognize pathogen-associated molecular patterns (PAMPs) like the viral RNA and/or damage-associated molecular patterns (DAMPs), including ATP, DNA and ASC oligomers¹. PRRs are expressed by a variety of cells, including the epithelial cells, that compose the barrier interface between the body and the external environment; phagocytes, primarily macrophages; dendritic cells, and many other types of cells. Upon PRR activation, downstream signalling cascades trigger the secretion of cytokines, mainly type I and III interferons (IFNs), and pro-inflammatory cytokines such as tumour necrosis factor alpha (TNF- α), and interleukin-1 (IL-1), IL-6, and IL-18. The secretion of such cytokines results in the stimulation of antiviral mechanisms in target cells and potentiates the adaptative immune response^{32,34}.

Interferons are a large family of structurally related cytokines that play an important role in viral defence. The most important interferons involved in the viral defence are type I, which include IFN- α and IFN- β . The type I interferons aimed to block the viral replication in both infected and uninfected neighbour cells by inducing an "antiviral state"³². Also, type I interferons sequester lymphocytes in lymph nodes, thus increasing the probability of encounter viral antigens. Type I interferons are also responsible for boosting the cytotoxicity of NK cells and CD8+ cytotoxic T lymphocytes (CTLs) and promote the differentiation of naive

T cells to the T_H1 subset of helper T cells, which results in enhanced innate and adaptive immune responses. Furthermore, they increase the expression of class I major histocompatibility complex (MHC) molecules, resulting in a higher probability of virally infected cells be recognized and eliminated. Type III interferons, which comprehend the IFN- γ , are mainly involved in the macrophage phagocytosis. As interferons represent one of the main barriers to viral infection, coronaviruses have evolved to overcome their protective function, by inhibiting IFN-I induction and signalling. In fact, recent studies demonstrated that COVID-19 patients underlying a severe disease status had remarkably impaired IFN-I levels in contrast to mild or moderate status³⁴⁻³⁶.

Among the cytokines produced after PRRs activation are interleukin-1 and 2 (IL-1 and 2), IL-6, granulocyte-colony-stimulating factor (G-CSF), IFN- γ inducible protein 10 (IP-10), monocyte chemoattractant protein 1 and 3 (MCP1 and 3), macrophage inflammatory protein 1 α (MIP-1 α) and tumour necrosis factor (TNF)³⁷. The secretion of such cytokines and chemokines results in the recruitment of blood leukocytes and plasma proteins to the sites of infection and injury, where they will exert its activity. These cytokines seem to be correlated with disease severity, becoming more elevated in patients with a worse prognosis³⁸.

The innate cells of the lymphoid lineage (ILCs) are effector cells which lack the expression of rearranged antigen receptors (T cell receptor (TCR), B cell receptor (BCR)). The ILCs can be divided in cytotoxic natural killer (NK) cells and non-cytotoxic helper ILCs, which include ILC1, ILC2, and ILC3³⁴. Multiple studies have described low numbers of NK cells in the peripheral blood of COVID-19 patients³⁹⁻⁴¹. These studies also correlate the reduced NK cells in the blood with disease severity. Moreover, several studies have described a decrease in maturation, recruitment, and cytotoxicity of NK cells³⁴. Several pathways may be contributing to this dysregulation observed on NK cells. TNF- α and IL-6 have been described as contributing to NK cell differentiation, although, so far, the effect of these cytokines in NK differentiation during SARS-CoV-2 infections have not been described^{34,37}. Together, these data suggest that several factors may be contributing to an impaired response of NK cells. Currently, ILCs functions in SARS-CoV-2 infections remain poorly investigated³⁴. Normally, all three subsets of ILCs are present in healthy lung tissue. ILC2s have an important role in restoration of the airway epithelium and oxygen saturation after respiratory infections. However, ILC2s also produce IL-13, contributing to the recruitment of macrophages. Indeed, ILCs are involved in the polarization of alveolar macrophages, either toward a M1-like phenotype (pro-inflammatory phenotype - ILC1 and ILC3) or a M2-like phenotype (anti-inflammatory phenotype - ILC2)⁴². Increased IL-13 levels were observed in COVID-19 patients

together with dysregulated macrophages response³⁷. However, further studies are needed to better understand the role of NK cells and ILCs during SARS-CoV-2 infections.

Generally, recruited cells are capable of clearing the infection in the lungs, and patients recover without needing medical support. However, growing evidence suggested that innate immune cell dysregulation may be involved in the hallmarks syndromes of COVID-19, such as acute respiratory distress syndrome (ARDS) and cytokine release syndrome (CRS), notwithstanding their critical role in early sensing and antiviral responses¹.

The mechanisms by SARS-CoV-2 subverts the innate immune response are yet to be studied. However, there have been described multiple mechanisms of evasion employed by the previous coronaviruses. Among them stand several viral proteins capable of antagonizing several signalling pathways, from PRR sensing and cytokine secretion to IFN signal transduction. Thus, it is very likely that some of these mechanisms are being employed by SARS-CoV-2³⁴.

2.3. Adaptive immune response

2.3.1. T cell-based immunity

To become activated, T lymphocytes, require the recognition of extracellular or intracellular antigens presented as peptides by the MHC. This interaction is accomplished by complex assembly signalling molecules, like CD4 and CD8 which are involved in the recognition of class II and class I MHC, respectively. CD4 positive T cells, when activated, become helper T cells producing cytokines, that regulate the immune response by recruiting other immune cells. One of the first responses of CD4+ T cells is the secretion of interleukin-2 (IL-2). IL-2 is a cytokine that acts on the antigen-activated lymphocytes and stimulates their proliferation. Moreover, some effector CD4+ T cells stay in the lymphoid organs and stimulate B cell responses. In contrast, CD8 positive T cells, when activated via TCR act as CTLs, delivering granzymes and perforins that will act on infected cells, eliminating the reservoirs of infection³².

Regarding SARS-CoV-2 infection, recent reports highlight the lymphopenia (drastically reduced numbers of both CD4 and CD8 T cells) observed in COVID-19 patients underlying moderate and severe disease status⁴³⁻⁴⁵. The extent of the lymphopenia observed in these studies seems to be correlated with disease severity and mortality. Further, patients with mild disease status typically present normal or slightly higher T cell counts⁴³⁻⁴⁵. Several mechanisms may be involved in the reduction of T cell numbers in blood samples from COVID-19 patients. Indeed, the levels of inflammatory cytokines, such as IL-6, IL-10, and TNF- α were correlated with the reduced number of T cells⁴⁶. Additionally, cytokines like IFN-I and TNF- α

may inhibit T cell attachment to endothelium and promote T cell retention in lymphoid organs. Some studies also suggest that lymphopenia can be correlated with the death of lymphocytes. Moreover, the recruitment of these cells to the sites of infection can also be correlated with the lymphopenia observed, as demonstrated by the increase of extensive lymphocyte infiltration in the lungs⁴⁷.

Although T cell activation is essential to control viral infection, a dysregulated response may contribute to COVID-19 immunopathology and disease severity. Zhou *et al.* reported high levels of GM-CSF+ CD4 T cells. These cells have been associated with poor outcomes in patients who developed sepsis. Moreover, low levels of regulatory T cells (Tregs) were observed in COVID-19 severe patients. Considering that Tregs have been shown to help resolve ARDS inflammation, low levels of these cells may be implicated in COVID-19 prognosis⁴³.

At this time, little is known about T cells' phenotype and functions during SARS-CoV-2 infections. Several reports showed that CD8 T cells seem to be more activated than CD4 T cells independent of COVID-19 disease severity⁴⁸. Moreover, it was also reported increased levels of PD-1 in COVID-19 patients. PD-1 expression is associated with T cell exhaustion⁴⁶. Additionally, several studies described elevated expression levels of various co-stimulatory and inhibitory molecules such as OX-40 and CD137, CTLA-4 and TIGIT, and NKG2a. Also, CD4 and CD8 T cell functions were shown to be reduced and dysregulated⁴⁹. CD8 T cells in severe COVID-19 appear less cytotoxic and CD4 T cells generate aberrant cytokine profiles, producing more than one cytokine as well as generally lower IFN- γ and TNF- α levels. In summary, T cells in critically ill patients with COVID-19 appear to be more activated and tend to exhaustion³⁴.

2.3.2. B cell-based immunity

The humoral immunity is mediated by secreted antibodies which are produced by the B cells of the lymphoid lineage. This type of immunity is essential for the elimination of cytopathic viruses and is a crucial part of the memory response that prevents reinfections³⁴.

SARS-CoV-2 kinetics of the antibody response is now reasonably well described, virus-specific IgM, IgG, and IgA, and neutralizing antibodies were detected globally in the days following infection⁵⁰. In most COVID-19 patients, seroconversion has been detected around the first week after the onset of symptoms⁵¹. In patients with SARS-CoV-2 infection, antibody responses typically arise against SARS-CoV-2 nucleocapsid protein and spike protein⁵². Neutralizing antibodies are detected in most tested patients around the 3 weeks of symptoms

onset^{53,54}. The main target of neutralizing antibodies is the RBD present in the spike protein⁵⁵. The interaction of these antibodies with the RBD blocks virus interaction with its host entry receptor, ACE2, and consequently viral replication. However, it seems that a small subset of patients did not develop long-lasting antibodies against SARS-CoV-2, whether these patients become susceptible to reinfections remains to be explored¹.

Until then, SARS-CoV-2 remains practically conserved, there are only known 4 rare alterations in the spike protein, although the RBD structure remains conserved¹. The low variability observed in SARS-CoV-2 structure remits for the low probability of escape to neutralization. Additionally, SARS-CoV-2 does not appear to have a mechanism to escape or prevent antibody neutralization⁵⁶. These results were supported by the high titres of neutralizing antibodies present in patients' plasma samples and previous results regarding SARS-CoV. Consequently, around the world, are being made huge efforts to develop therapeutic antibodies against SARS-CoV-2. Several approaches are being explored for this purpose, such as antibody phage libraries, traditional mouse immunizations, cloning of B cell sequences from COVID-19 convalescent patients among other strategies¹. However, therapeutic antibodies must be carefully selected due to the potential unwanted side effects. Previous studies on SARS-CoV showed that neutralizing antibodies can potentially augment severe lung injury by exacerbating inflammatory responses, by inducing the expression of pro-inflammatory factors, including IL-8 and MCP1, and activating phagocytosis by macrophages^{57,58}. Therefore, its important to study not only the neutralizing activity of the potential therapeutic antibodies but also its pro-inflammatory activity.

3. THESIS AIM

Worldwide, the continuous spread of COVID-19 has become a huge public health problem with social, economic, and political devastating consequences. Because of its recent emergence, there is a large lack of information regarding viral host interaction and evasion of host immune response. Consequently, there is an urgent need to understand the underlying disease mechanisms, since they will provide vital information for the management and treatment of the disease, including the development of new effective therapies.

Therefore, the aim of this thesis was to characterize the immune responses triggered by SARS-CoV-2 and find patterns associated with the quality and amplitude of the immune response in severe COVID-19 patients. Thus, to achieve this goal, the following specific objectives were proposed:

- 1) Longitudinal analysis of antibody responses chiefly:
 - a. Which antibody classe(s) are involved in humoral response?
 - b. How do antibody titers vary throughout hospitalization stay?
 - c. How do neutralizing antibody responses developed throughout time?
- 2) Characterization of antibody response SARS-CoV-2 RBD.
 - a. Which RBD epitopes are the most immunogenic and which are likely involved in viral neutralization?
- 3) Analysis of the variation of cytokine/chemokine immune responses over time.
 - a. Which cytokines and chemokines are most altered relative to baseline (healthy control group)?
 - b. Are there cytokines pattern(s) associated with the patient's status that can be correlated with the clinical outcome?

Altogether, these data may contribute for the development of clinical predictive models for COVID-19 that estimate which patients most likely develop severe clinical outcomes. Furthermore, the cytokine signature responses may give important hints to clinicians in order to modulate the inflammatory immune response in early disease stage avoiding bad clinical trajectories and deaths.

CHAPTER II: Materials and Methods

1) Study design and human samples

Study participants were recruited at the Hospital Curry Cabral in Lisbon from 14 March to 14 June 2020. All eligible participants had a SARS-CoV-2 infection, confirmed by RT-PCR, and characterized by a severe clinical outcome, which resulted in their admission to the intensive care unit (ICU) of the hospital. Demographic data and clinical characteristics of the participants are shown in Extended Data Table 1. For the cohort follow-up, serum samples were collected every 3 days from the admission on UCI until discharge. Approximately 4 samples were obtained per patient.

Blood samples were collected into BD vacutainer EDTA blood collection tubes and centrifuged at $2000 \times g$ for 10 minutes, allowing separation of plasma from the other blood components (platelets, and red and white blood cells). Following centrifugation, plasma was aliquoted and stored at -80°C for later use.

2) Enzyme-linked immunosorbent assay (ELISA)

a. Detection of IgG's and IgM's against SARS-CoV-2 by indirect ELISA

Spike S1 and S2

In order to screen plasma samples for their reactivity against SARS-CoV-2 antigens, the recombinant SARS-CoV-2 spike S1 or S2 subunit proteins (Acro Biosystems) were used and immobilized onto high binding polystyrene 96 well microplates (Corning), overnight at 4°C , diluted at $1.25 \mu\text{g}/\text{mL}$ in phosphate buffer saline (PBS) at pH 7.4. On the following day, plates were washed once with $150 \mu\text{L}/\text{well}$ of Wash Buffer (PBS pH 7.2, containing 0.05% Tween-20), to remove unbound proteins. Plates were then blocked, for 2 h at 37°C , with 3% BSA dissolved in PBS containing 0.1% Tween-20, to prevent unspecific binding of proteins to the plate. After washing (3x) with Wash Buffer, $50 \mu\text{L}$ of 1:50 diluted serum samples were added in duplicate to plates and incubated under gentle agitation for 1 h at 24°C . Following a washing cycle, goat anti-human IgG Fc horseradish peroxidase (HRP) conjugated (abcam) and/or goat anti-human IgM μ chain HRP conjugated (abcam) were added at a 1:20,000 dilution and 1:250,000, respectively, and incubated for 1 h at 24°C . After washing, the signal was developed using an ultrasensitive TMB substrate and plates incubated in the dark. The reaction was stopped after 10 minutes with 0.5 M sulfuric acid and optical density (OD) values were read at 450 nm using a plate reader (Multiskan FC, ThermoFisher Scientific).

Antibody levels were presented as the OD at 450 nm divided by the cut-off point (CP) of the assay ($\text{OD}_{450\text{nm}}/\text{CP}$). Samples with $\text{OD}_{450\text{nm}}/\text{CP}$ greater than or equal to 1 were defined as positive and samples with $\text{OD}_{450\text{nm}}/\text{CP}$ less than 1 were defined as negative.

Nucleocapsid

To detect antibodies against the SARS-CoV-2 nucleocapsid, ELISA plates were coated with 1 µg/mL of recombinant SARS-CoV-2 nucleocapsid protein (abcam) in PBS at pH 7.4 and incubated overnight at 4 °C. The following protocol steps were performed as described above.

b. Screening of IgA antibodies against SARS-CoV-2

ELISA plates were coated with a capture mouse monoclonal antibody to human IgA (abcam) at 2 µg/mL and incubated overnight at 4 °C. After standard washing and blocking, 50 µL of 1:10 diluted plasma samples were added in duplicate to the plates. Following 2 h of incubation at 24 °C, plates were washed and 50 µL/well of biotinylated SARS-CoV-2 spike S1 or nucleocapsid protein (Acro Biosystems) were added at a 1:100 or 1:10,000 dilution, respectively. Past 1 h incubation and new washing cycle, 50 µL of Streptavidin HRP conjugate at a 1:10,000 dilution was added to each well for 1 h at 24 °C. TMB substrate was added, and after 15 min, the reaction was stopped, and the absorbance was read at 450 nm.

3) Cross-reactivity of antigens from nCoV-NL63 and the SARS-CoV

ELISA plates were initially coated with 1 µg/mL of recombinant nCoV-NL63 S1+S2 ectodomain (ECD) and the SARS-CoV nucleocapsid (Abcam) in PBS at pH 7.4. Following overnight incubation, IgG antibodies present in patients' plasma samples and healthy controls were detected as described above.

4) Surrogate virus neutralization assay

Reconstituted recombinant SARS-CoV-2 spike S1 was immobilized onto ELISA 96 well microplates at 1 µg/mL in PBS, pH7.4, overnight at 4 °C. On the next day, and after standard washing and blocking, the recombinant human angiotensin converting enzyme 2 (ACE2) was diluted at 100 ng/mL (two-fold final dilution) in diluent buffer and added to microplate. Plasma samples were immediately transferred from low binding dilution plates to ELISA microplate, following the serial three-fold scheme dilution starting from 1:3.3 down to 1:2430. Samples were incubated 1 h at 24 °C with agitation (500 rpm). After washing, streptavidin HRP conjugate was diluted at 1:1000 in diluent buffer, added to microplate and then incubated again for 1 h at 24 °C with agitation. Finally, the signal was developed by adding ultrasensitive TMB substrate to wells and plates incubated in the dark. Reactions were stopped 10 minutes later by adding 0.5 M sulfuric acid to wells and the absorbance read at 450 nm.

A commercial neutralizing IgG antibody against the SARS-CoV-2 spike S1 produced in mouse was used as a positive control, whereas plasma samples from healthy volunteers, serologically tested for SARS-CoV-2 spike were used as negative controls and allowed to set a cut-point.

The inhibition percentage (%) for each sample was calculated according to the following metric: $(1 - \text{sample optical density value} / \text{negative control optical density value}) \times 100$. For determination of neutralizing titers, the IC_{50} was calculated for each potential neutralizing plasma sample. Optical densities from plasma dilutions were used to calculate a dose response curve by making a logistic regression with software available on GraphPad Prism version 8.

5) Epitope mapping

A linear peptide library comprising nineteen peptides, each one composed by 20 residues and with an overlap of 10 amino acids between successive peptides, were chemically synthesized (ProteoGenix SAS) to cover the amino acid sequence of the Region Binding Domain (RBD) of the spike S1 protein (Extended Data Table 2 and Extended Data Fig.1). A hemagglutinin (HA) peptide composed of 9 amino acids attached to biotin at the N-terminus was used as a positive control of the plate.

ELISA plates were coated with 10 $\mu\text{g/ml}$ of each peptide in carbonate buffer pH 9.6 and kept overnight at 4 $^{\circ}\text{C}$. Plates were then washed once with wash buffer, to remove unbound peptides, and blocked for 1 hour 30 minutes at 37 $^{\circ}\text{C}$ with 1% Casein (Sigma-Aldrich) in PBS containing 0.1% tween 20. On the next day, plates were washed 3 times with wash buffer and plasma samples diluted at 1:100 in diluent buffer were added in duplicate to the microplates. For each plate, a positive control diluted at 1:1000 (Abcam) in diluent buffer was also added previously. After 1 h incubation at 24 $^{\circ}\text{C}$, plates were washed and incubated with goat anti-human IgG Fc horseradish peroxidase (HRP) conjugated (abcam) at a 1:20,000 dilution. Following 1 h incubation at 24 $^{\circ}\text{C}$, plates were washed, and the signal was developed using an ultrasensitive TMB substrate and plates incubated in the dark. The reaction was stopped 10 minutes later by adding 0.5 M sulfuric acid to wells and the absorbance read at 450nm.

The binding epitope data was submitted to the ClustVis⁵⁹ software. Data were pre-processed applying a new variance scale and correlations between variables were performed through Pearson's rank test.

6) Cytokine and Chemokine Protein Quantification by Multiplex ELISA

Multiplex ELISA is a technique that uses color-coded magnetic beads to detect and measure simultaneously multiple analytes in a single experiment. Briefly, each bead is associated with a specific dye concentration and a single target, which is determined by the cytokine-specific capture antibody attached to the bead. Once the analyte is captured by the bead, a biotinylated detection antibody is introduced. The reaction mixture is then incubated with streptavidin-phycoerythrin conjugate (reporter molecule) to complete the reaction and allow the detection of the analyte by the Luminex equipment.

The human plasma GM-CSF, TNF- α , TNF- β , IFN- γ , IL-1 β , IL-2, IL-4, IL-5, IL-6, IL-8, IL-9, IL-10, IL12p70, IL-13, IL-15, IL-17a, IL-17E, IL-17F, IL-21, IL-22, IL-23, IL-27, IL-28a, IL-31, IL-33 and MIP3a/CCL20 levels were quantified using multiplex cytokine/chemokines HTH17MAG14K and HCYTA-60K-13 (Millipore) performed with collaboration of technical personnel from ARIUM Diagnostic solutions SA. Serum levels of TGF- β 1 were measured using the Human TGF beta 1 ELISA kit (Invitrogen).

7) Statistical analysis

Statistical analyses were performed using an unpaired two-tailed Student's t-test in order to compare the differences between groups (patients serum samples vs. healthy serum samples). A p -value of <0.05 was considered statistically significant. Statistical analyses were performed using GraphPad Prism 8.0. Correlations of SARS-CoV variables were analyzed using Pearson correlation coefficients.

CHAPTER III: Results

1. Characterization of Patients

Between 14th April through 14th June of 2020, 17 eligible participants, with ages between 18 to 83 years old (medium age, 60.9 years old), were enrolled in a prospective, longitudinal study with the goal to characterize the immune responses triggered by SARS-CoV-2 and find patterns associated with the quality and amplitude of the immune response. All the patients were infected with SARS-CoV-2, confirmed by RT-PCR, and characterized by a severe clinical outcome, which resulted in their admission to the intensive care unit (ICU) at Curry Cabral Hospital. Patient demographics and clinical characteristics are shown in Extended Data Table 1. Of these patients, 76.5% were male.

The mean days from symptom onset (DFSO) was approximately 13.8 days (range, 2–33 days) before ICU admission. The most common symptoms were fever (88%), cough (70%), and dyspnoea (47%). In addition, less common symptoms like vomiting and diarrhea were presented in 23% of the patients; nausea, abdominal pain, and hypogeusia were displayed in 12%; and sore throat, anosmia, and headache in 6%. Baseline comorbidities were frequent in 82% of patients. High blood pressure (64%), diabetes (53%), and obesity (18%) were the most prominent risk factors among the cohort population.

Regarding the therapeutic exposure regimens, vasopressors and corticoids were the most used to treat IC-patients, representing 76% and 41%, respectively. In addition, 47% of patients were treated with remdesivir, while only 12% of patients received tocilizumab. During the hospitalization time (range between 2 and 32 days), patient's blood samples were collected every 3 days. Of the total number of patients admitted to the study, 15 were discharged from the ICU after their clinical condition improved and 2 deceased.

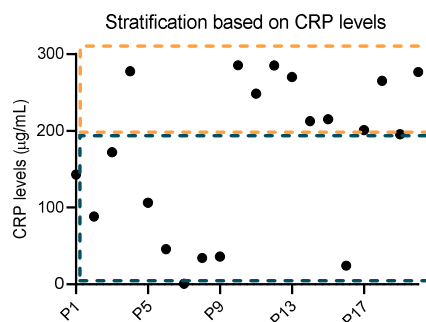


Figure 4| COVID-19 patients stratification based on CRP blood levels. Patients with CRP above 200 µg/mL (orange) were classified as critical, while patients with CRP levels below or equal to 200 µg/mL (blue) were classified as severe.

The cohort was stratified according to C-reactive protein (CRP) levels, *i.e.*, patients with CRP above 200 µg/mL were classified as critical (n=10), while patients with CRP levels below or equal to 200 µg/mL were classified as severe (n=7). The threshold was defined based on the distribution of data points observed when representing the CRP levels on admission for all patients (Fig.4).

The median age was 55 years in patients with severe disease status whereas for the critical subgroup was 63 years. In contrast, the median age in non-survival patients was 83 years. In addition, no significant differences in both groups were observed in male and female ratios. However, of note, all non-survival patients were male. Besides, it was observed that patients with severe progression underwent a greater number of therapeutic regimens. Furthermore, no significant associations were found between the remaining clinical parameters and stratified patients (Extended Data Fig.1).

2. Characterization of antibody responses to SARS-CoV-2

To determine the nature of the antibody response elicited by the SARS-CoV-2 infection, we develop two different versions of an enzyme-linked immunosorbent assay (ELISA). Therefore, to screen IgM and IgG antibody responses to SARS-CoV-2, an indirect ELISA was developed, using the recombinant SARS-CoV-2 spike S1 and S2 subunits along with the nucleocapsid protein as coating antigens. For the detection and titration of plasma IgA antibodies, a sandwich ELISA was chosen instead of the indirect format, as the higher sensitivity of the former allows to detect low levels of circulating plasma IgA antibodies against SARS-CoV-2. All reagents, buffers and conditions were tested following a chessboard approach in order to achieve the best signal-to-noise ratio, *i.e.*, low background and high sensitivity and specificity.

To validate the performance of the developed assays, we tested plasma samples from SARS-CoV-2 patients and a total of 50 plasma samples from healthy volunteers negative for SARS-CoV-2 infection (previously confirmed by RT-qPCR).

The detected signals for each class of SARS-CoV-2 antigen-specific antibodies are summarized in Fig.5 The spike S1-specific IgA, IgM, and IgG assays showed diagnostic sensitivities of 81.25%, 100%, and 100%, and specificities of 100%, 94.75%, and 95.45%, respectively. The sensitivities, specificities, and overall agreements of the nucleocapsid-specific IgA (se=93.75%, sp=87.10%), IgM (se=87.50%, sp=80%), or IgG (se=100%, sp=96.43%) assays are also summarized in Fig.5 A and C. Finally, spike S2-specific IgM and IgG assays showed a sensitivity of 93.75%, and 81.25%, and specificities of 76.32% and

61.25%. The selection of cut-point was based on a high sensitivity and specificity calculated by a receiver operating area under the curve (ROC AUC) (Fig.5A).

To detect cross reactivity between SARS-CoV-2 and other seasonal coronaviruses, we performed ELISAs coated with recombinant nCoV-NL63 S1+S2 ECD and the SARS-CoV nucleocapsid. The detected signals were plotted in Fig.5D. The sensitivities and specificities are summarized in Fig.5B. Negative controls and patient's plasma samples did not showed reactivity against these proteins.

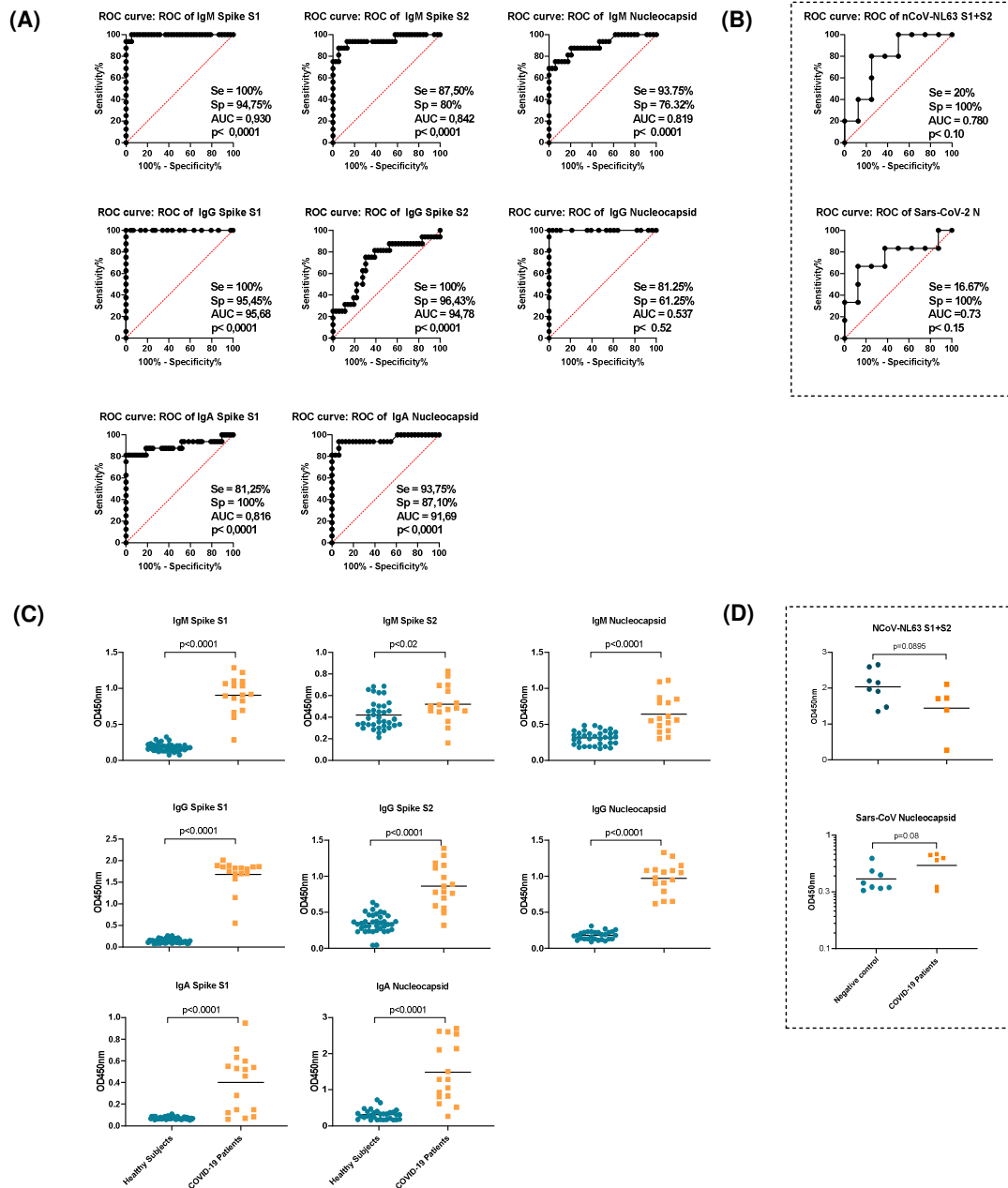


Figure 5 | Characterization of ELISA immunoassay performance. (A) Receiver-operating characteristic (ROC) analysis for evaluation of ELISA to detect reactivity to SARS-CoV 2 antigens and (B) cross-reactivity against other SARSs (C) Reactivity and (D) cross-reactivity of control and SARS-CoV-2 convalescent plasma to different antigens. Each dot represents a separate time point per subject (Healthy subjects, $n = 50$; COVID-19 patients, $n = 17$). Black lines indicate mean values. Statistical analyses were performed using an unpaired two-tailed Student's t-test. (se- sensitivity; sp- specificity; AUC- area under the curve)

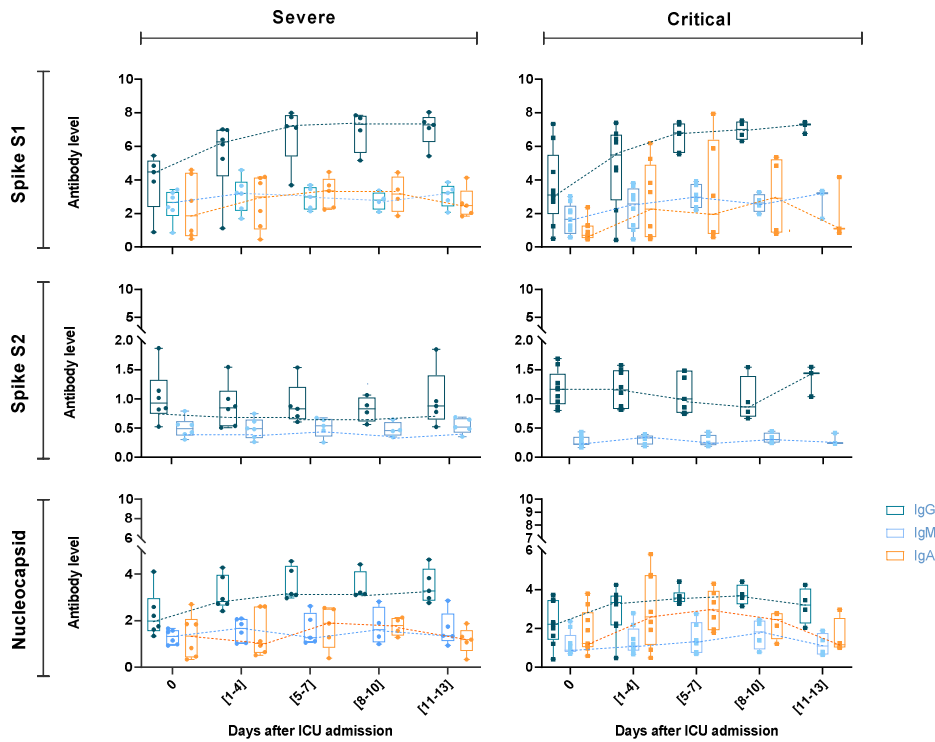
a. Longitudinal analysis of the antibody responses

In order to evaluate the kinetic of antibody response during ICU stay time, plasma samples were collected every 3 days and screened for several antibody classes (IgA, IgM, and IgG) against SARS-CoV-2 spike S1 and S2 subunits, and nucleocapsid protein (Extended Data Fig.2).

We did not find significant differences between severe and critical patient groups when analyzing spike S1-, S2-, and nucleocapsid-specific IgG and IgM antibodies during UCI stay time (Extended Data Fig.3). In addition, we found that the levels of spike S1-specific IgM and IgG antibodies were greatly higher when compared to nucleocapsid-specific antibodies. Curiously, we did not find spike S2-specific IgG and IgM antibody responses (Fig.6A). Our observations showed that IgG antibody responses against spike S1 and nucleocapsid were already 4-fold and 2-fold increased relative to background on early stage of hospitalization (on admission). Nonetheless, IgG antibody titers continued to increase until approximately day 6 at ICU, after which titers reached a plateau (7-fold higher than background assay) (Fig.6A). In the case of IgM antibody response, the levels remained constant during ICU stay time. The spike S1-specific IgM antibodies were maintained at a 2-fold increasing regarding the control baseline, while nucleocapsid-specific IgM was maintained close to the background (Fig.6A). In the case of spike S1- and nucleocapsid-specific IgA levels, we observed a great variation between severe and critical patients. S1- and nucleocapsid-specific IgA antibody levels increased over time until reaching a peak around day 6 of ICU admission, followed by a rapid decline close to the cut-point value in both severe and critical groups (Fig.6A, Extended Data Fig.2). However, the variation in the antibody responses was extremely disparate in critical patients (more than 8-fold). Nonetheless, it is important to note that the non-survival COVID-19 patients in this study failed to develop high titre serum antibody response against the several SARS-CoV-2 proteins tested (spike S1, S2, and nucleocapsid) (Data not shown).

In order to determine associations between the variables antibody levels and RCP levels on admission, we performed several correlations as shown in Fig.6B. A strong positive correlation was observed between anti-spike S1 IgG and CRP levels in the severe group ($r=0.875$, $p=0.05$). Furthermore, in the critical group, we observed moderate negative correlations between IgG vs. CRP levels ($r=-0.395$, $p=0.292$) and IgA vs. CRP levels ($r=-0.447$, $p=0.228$), though not statistically significant. In addition, all remaining plots did not show any significative correlations between variables.

(A)



(B)

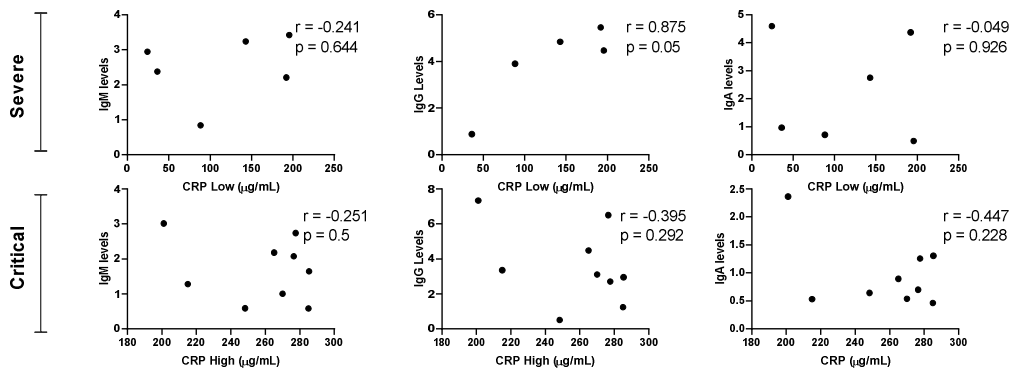


Figure 6| Evaluation of the antibody responses to SARS-CoV-2 in IC- patients. (A) Comparison of different classes of antibodies between severe and critical COVID-19 patients at different time points after ICU admission. The boxplots show medians (middle line) and third and first quartiles (boxes), while the whiskers show the minimum and maximum values observed. Antibody levels were presented as the absorbance at 450 nm divided by the cut point (Abs/CP). Abs/CP ≥ 1 was defined as positive and Abs/CP < 1 as negative. **(B)** Scatter plots showing the correlations between CRP levels with all denoted antibody classes tested in critical and severe groups. Spearman's was used to evaluate the correlations.

b. Characterization of neutralizing antibody responses

In order to evaluate the quality of the humoral immune responses in the cohort population, we analyzed the neutralizing antibody (Nab) responses in the course of SARS-CoV-2 infection. Currently, the gold standard assay to determine the presence of neutralizing antibodies (NABs) against SARS-CoV-2 is a virus neutralizing assay that explores the molecular mechanism of virus entry into the cell. This assay presents a main biosafety-related issue due to virus handling on a biosafety level 3 laboratory and the subsequent slowdown of the work process⁶⁰.

Here, we implemented a surrogate virus neutralizing assay as described by Wah Tan *et al.* (2020)⁶⁰. Briefly, our assay relies on the same principle as described by conventional virus neutralizing assay but uses the SARS-CoV-2 spike S1 subunit protein, immobilized to a polystyrene microplate, instead of the authentic virus. The signal inhibition quantifies the presence of NABs in percentage when compared to an interaction control, *i.e.*, interaction established between SARS-CoV-2 spike S1 and human biotinylated ACE2 only. The test, which has been established, achieves 98% specificity and 100% sensitivity as attested in Fig. 7.

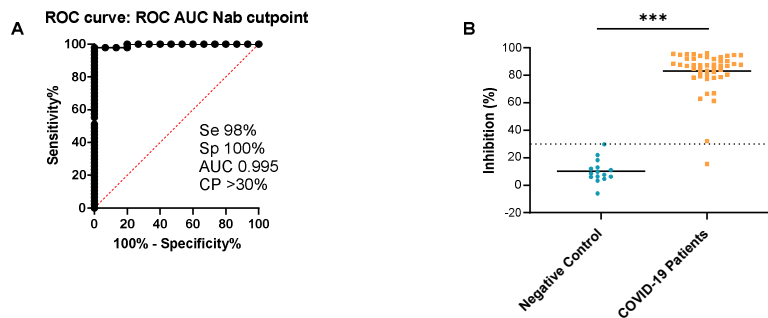


Figure 7 | Validation of in vitro neutralizing antibody assay to Sars-CoV-2. (A) Determination of sensitivity (Se), specificity (Sp), and cutpoint by ROC approach. Cutpoint (CP) was determined by comparing mean inhibition % of (Nab) sera samples from a control group composed by healthy age matched volunteers (N=15) and of COVID-19 patient sera samples (N=47). **(B)** Unpaired two-tailed student's t test was used between the two datasets, p-value <0.05. The inhibition (%) for each sample was calculated according to the following metric: $(1 - \text{sample optical density value} / \text{negative control optical density value}) \times 100$. AUC Area Under the Curve; *** Significance below $p < 0.0005$.

We observed that on early stage of hospitalization, patients already presented low titers of NABs, however these titers were still relatively low ($IC_{50} = 10$). It is noteworthy that patients with severe clinical state showed a slight increase in Nab titers in relation to patients with critical status. On day 6 of hospitalization (middle time point of follow-up), both NAb titer responses increased markedly, yet more pronounced for severe patient subset. In the last days of hospitalization, the patients maintained the NAb titers constant but still showing a slight

increase in critical subset. Overall, and during hospitalization in intensive care unit, severe patients showed a neutralizing antibody kinetic activity identical to critical patients but presented always a better Nab activity (Fig.8A)

Furthermore, as depicted in Fig.8, we have identified strong negative correlations between neutralizing titers measured on the last time point with CRP in both patients' group. Thus, the severe group presented a Pearson's coefficient of 0.76 ($p=0.08$) whereas critical patients presented a coefficient of approximately 0.6 ($p=0.096$). In addition, we also detected a strong association between Nab titers vs. S1-specific IgG antibody titers in critical patients ($r=0.6$; $p<0.0005$). For the IgA to IgG levels' ratio, the associations were weaker ranging between $r=0.26$ for low CRP and $r=0.4$ for critical patients, but significant in the severe group ($p=0.009$). (Fig.8B, C, and D)

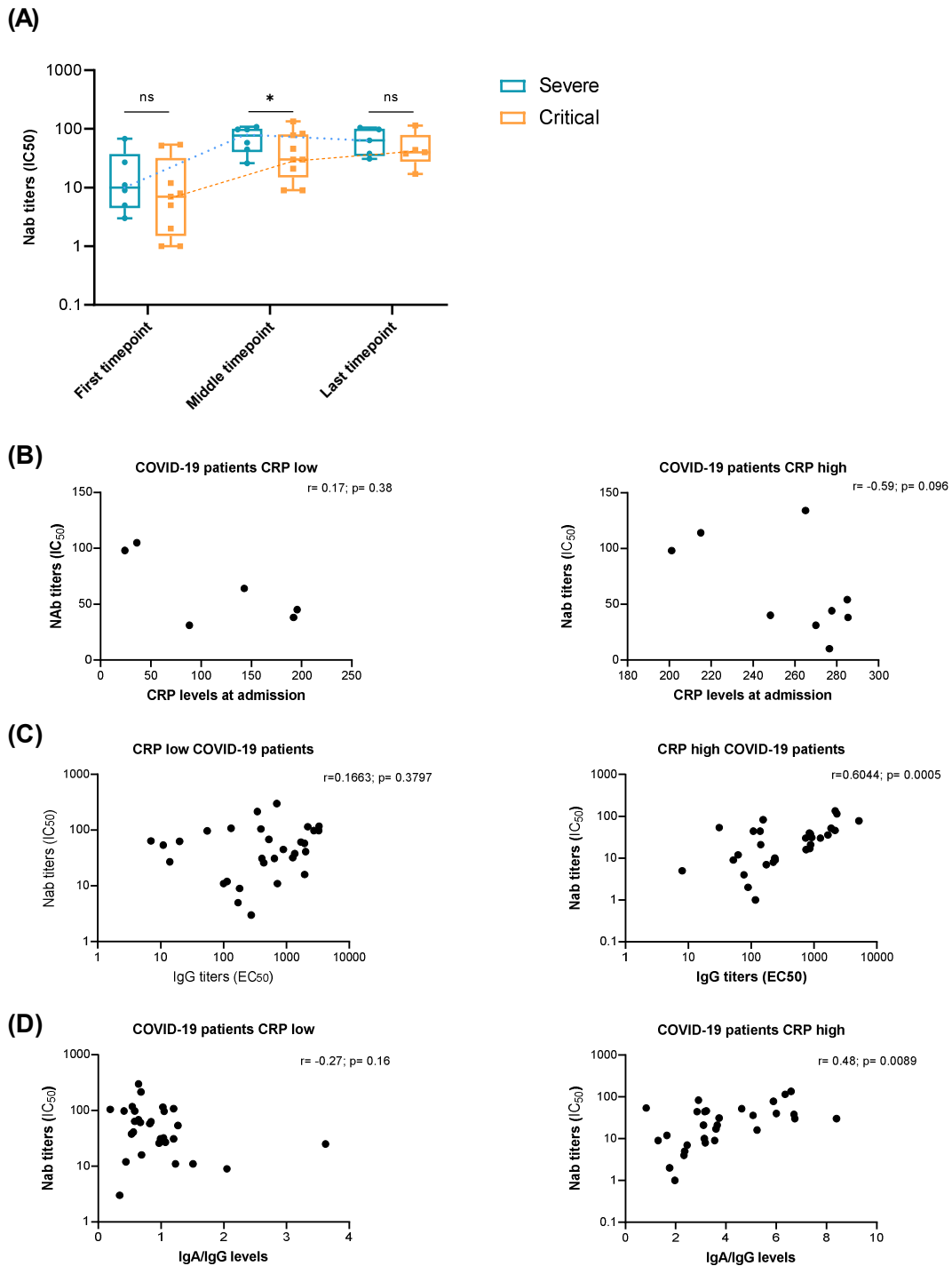


Figure 8 | Assessment of Nab titers overtime and correlations with CRP, IgG, and IgA levels in COVID-19 ICU- patients (A), COVID-19 patients are represented by severe (blue dots) and critical (red dots) across three time points. Middle solid lines represent the median of Nab titer values and the upper and lower boxplot represent the 3rd and 1st quartiles while the whiskers show the maximum and minimum values. A student's t test was performed to determine the differences between datasets (severe vs critical). (B), Correlations of Nab titers between CRP low and high levels (all data points were used) (C) with IgG levels and (D), IgA divided by IgG levels. Spearman's rank test was used to performed correlations between variables. IC₅₀ - half maximal inhibitory concentration, EC₅₀ - half maximal effective concentration. * denotes p-value <0.05.

3. Characterization of antibody response to RBD epitopes from SARS-CoV-2

In order to study the reactivity of COVID-19 patients' plasma samples against the SARS-CoV-2 RBD domain, we designed a peptide library composed of 19 overlapping peptides mimicking the SARS-CoV-2 RBD epitopes. Each peptide composition is shown in Extended Data Table 1 and a schematic representation in Fig 9. The extension of the antigenic response is reflected by the intensity of the heatmap shown in Figure 10. Dark blue indicates low binding to the respective epitope while yellow to red indicates moderate to high binding.

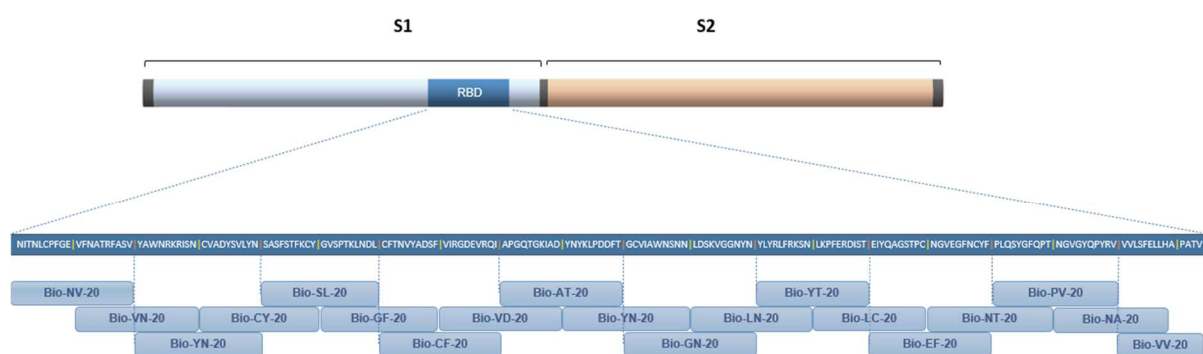


Figure 9| Schematic representation of the synthesized peptides covering the RBD domain. S1 subunit is shown in light blue and the RBD domain in dark blue, while S2 subunit is shown in orange. Each peptide is composed by 20 residues with an overlap of 10 amino acids between successive peptides.

As observed in Figure 10, ten of these peptides (52%) showed moderate to high reactivity to ICU patients' plasma samples. Therefore, they were grouped in 2 clusters: clusters 1, composed of 6 peptides (Bio- Bio-NV-20, Bio-VN-20, Bio-YN-20, Bio-CY-20, Bio-SL-20, Bio-GF-20), and cluster 2, composed of 4 peptides (Bio-NT-20, Bio-PV-20, Bio-NA-20, Bio-VV-20). As observed in Fig.9, cluster 1 and 2 were located at N- and C-terminal of the RBD domain, respectively. The remaining peptides, which were located between the two clusters, showed very despicable immunoreactivity. Comparing the reactivity among the two clusters we observed that cluster 2 showed highly increased reactivity compared with cluster 1. We also observe that in cluster 2, a peptide (Bio-NT-20) stands out with increased reactivity compared to the remaining.

Cluster 2 peptides, in the three-dimensional structure, are located in the RBD site of interaction with its receptor, the ACE2, whereas peptides of cluster 1 are located in the opposite location of the RBD-ACE2 site of interaction (Fig.11). Peptides with low reactivity are located in an interior location in the RBD three-dimensional structure (data not shown).

Moreover, our results demonstrate that all ICU patients developed antibodies against the RBD epitopes (Fig.10). Further, when analyzing the response among the several stratifications groups (severe and critical), we did not find significant differences in the peptides immunoreactivity. However, we noticed that in both stratification groups, some patients (Y002, Y011, Y016, Y019, and Y020) exhibited a distinct pattern of reactivity across RBD epitopes. Regarding the results obtained in non-survival patients, we could not identify meaningful differences that could explain the outcome observed in these patients.

In order to evaluate the longitudinal variation reactivity of antibodies along, we analyzed plasma samples collected at initial, middle, and final ICU stay times, when possible. Our data demonstrated that there was no variation in the reactive peptides (Fig.10). Clusters 1 and 2 continue to have superior reactivity compared with the remaining ones. However, we noted an increase in reactivity along ICU stay time in almost all patients.

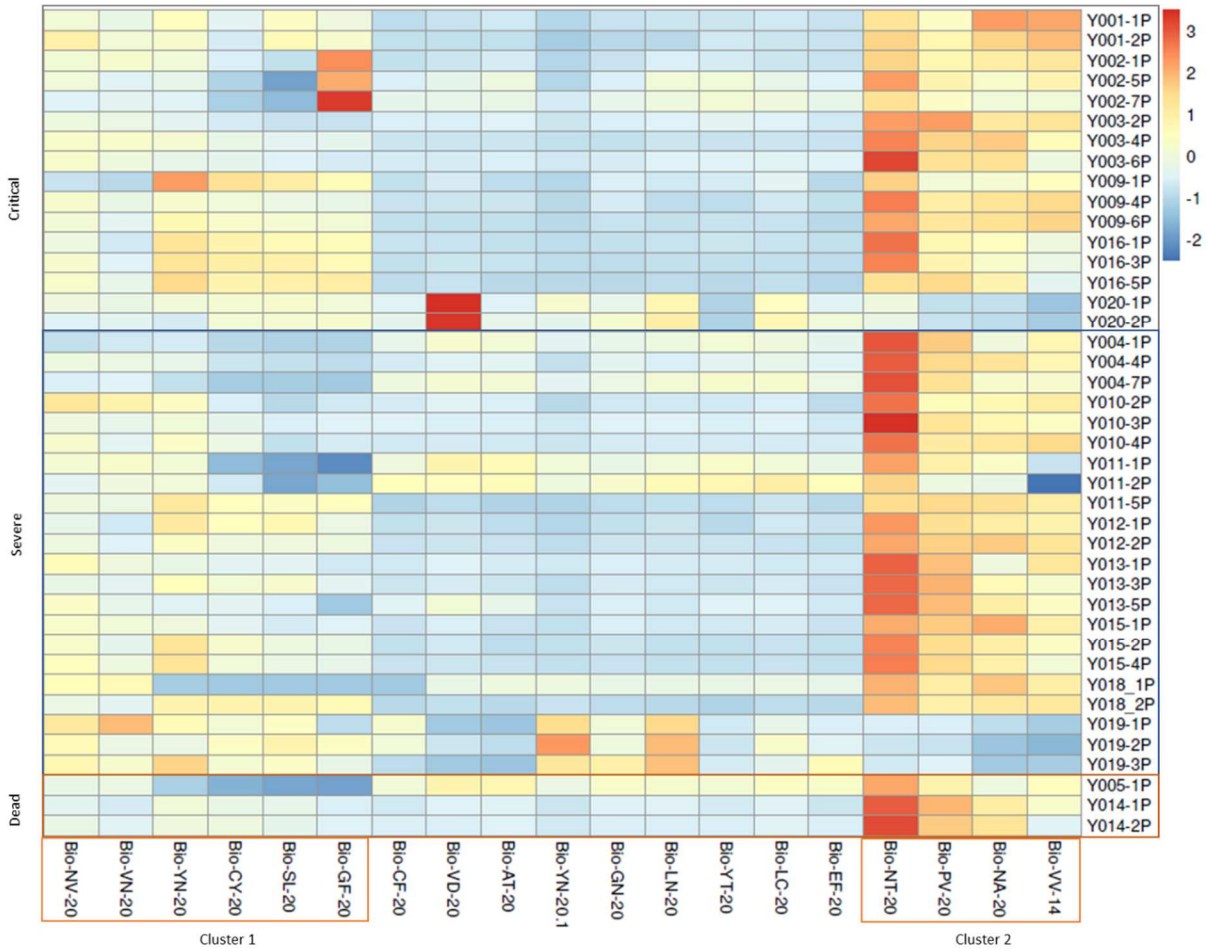


Figure 10| SARS-CoV-2 RBD immunoreactivity in COVID-19 patients. The heatmap summarizes the immunoreactivity of SARS-CoV-2 RBD epitopes against IgG antibodies present in COVID-19 patients plasma samples, obtained at different times after ICU admission. Dark blue indicates low binding to the respective epitope while yellow to red indicates moderate to high binding.

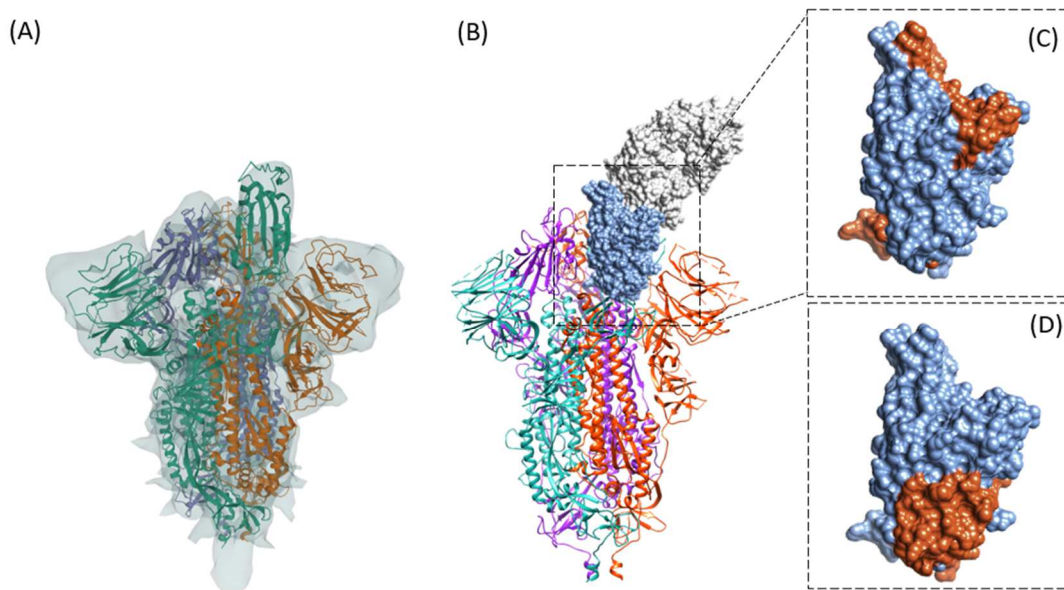


Figure 11| Three-dimensional structure of Spike protein of SARS-CoV-2 and schematic representation of clusters 1 and 2. Surface and ribbon diagram of SARS-CoV-2 spike protein (A). Ribbon diagram of SARS-CoV-2 spike protein showing the interaction between RBD (blue) and its receptor, angiotensin-converting enzyme 2 (ACE2), represented in grey (B). The orange highlighted regions show the location of the most immunogenic peptides, which were grouped in cluster 1 (D) and cluster 2 (C). Cluster 1 is composed of 6 peptides (Bio-NV-20, Bio-VN-20, Bio-YN-20, Bio-CY-20, Bio-SL-20, Bio-GF-20) while cluster 2 is composed of 4 peptides (Bio-NT-20, Bio-PV-20, Bio-NA-20, Bio-VV-20). Adapted from Protein Data Bank ID 7A94 and 7VXX.

4. Cytokine/chemokine immune responses

In order to compare the cytokine expression levels between COVID-19 patients and healthy subjects (control group), we analyzed the cytokine levels in plasma samples collected on admission, mid-, and end-hospitalization at ICU. Data were generated by a multiplex approach that enables to reduce the variability between each cytokine readout. Data obtained were analyzed using all data sets to represent the variations observed within COVID-19 patients in contrast to healthy subjects. The results are shown in the heatmap of Fig.12. Cytokine expression levels are represented by a colour scale, ranging from intense red for the lowest to green for the highest expression levels.

The primary focus of our analysis was to find a cytokine expression pattern(s) that could discriminate between patients with COVID-19 and healthy individuals. Thus, we identified a COVID-19 signature characterized by an upregulation of several inflammatory cytokines and chemokines in both patient groups of which we highlight the following: GM-CSF, TNF- α , IFN- γ , IL-1 β , IL-5, IL-6, IL-8, IL-15, TGF- β , IL-27, and MIP3a/CCL20 (Fig.12, Extended Data Table 3).

Notably, in patients that had succumbed to COVID-19 (Y005 and Y014) we identified a divergent cytokine profile. In patient Y014, most of the cytokines, such as TNF- β , IFN- γ , IL-4, IL-5, IL-6, IL-8, IL-9, IL-10, IL-12p70, IL-15, TGF- β , IL-27, IL-28a, and MIP3a were highly altered (Fig.12). Contrasting, a weak cytokine response was observed in patient Y005. Of note, IL-10 is extremely high in this patient. Moreover, patient Y009 has an altered cytokine profile; however, the signature did not correlate with COVID-19 itself, but with the underlying chronic liver disease. Additionally, patients with moderate disease (Y006 and Y007) did not show significant differences in the expression levels of IL-6, IL-8 and MIP3a relative to control group (Fig.12).



Figure 12| Dysregulated cytokine responses in ICU COVID-19 patients. Heat map reveals a cytokine signature of immune responses associated to COVID-19 patients. Cytokine data were normalized according to variance measured on each individual cytokine dataset. Cytokine expression levels are represented by a color scale, ranging from intense red for the lowest to green for the highest expression levels.

Longitudinal cytokines variation, measured in terms of days after ICU admission, indicated the major differences observed between patients with severe or critical disease (Fig.13). In the first days after ICU admission, patients with severe or moderate disease displayed similar levels of the cytokines and chemokines characteristic of the overall core COVID-19 signature described above. Overall, we did not observe significant differences in the expression of inflammatory markers along disease progression between patients who exhibit moderate vs. severe symptoms of COVID-19. Nonetheless, TNF- α , IL-6, IL-27, and MIP3a levels increased over ICU stay time in patients with critical disease but declined in patients with severe disease. Furthermore, the remaining cytokines tended to decline steadily over time, approaching the levels of healthy individuals, at the time of discharge.

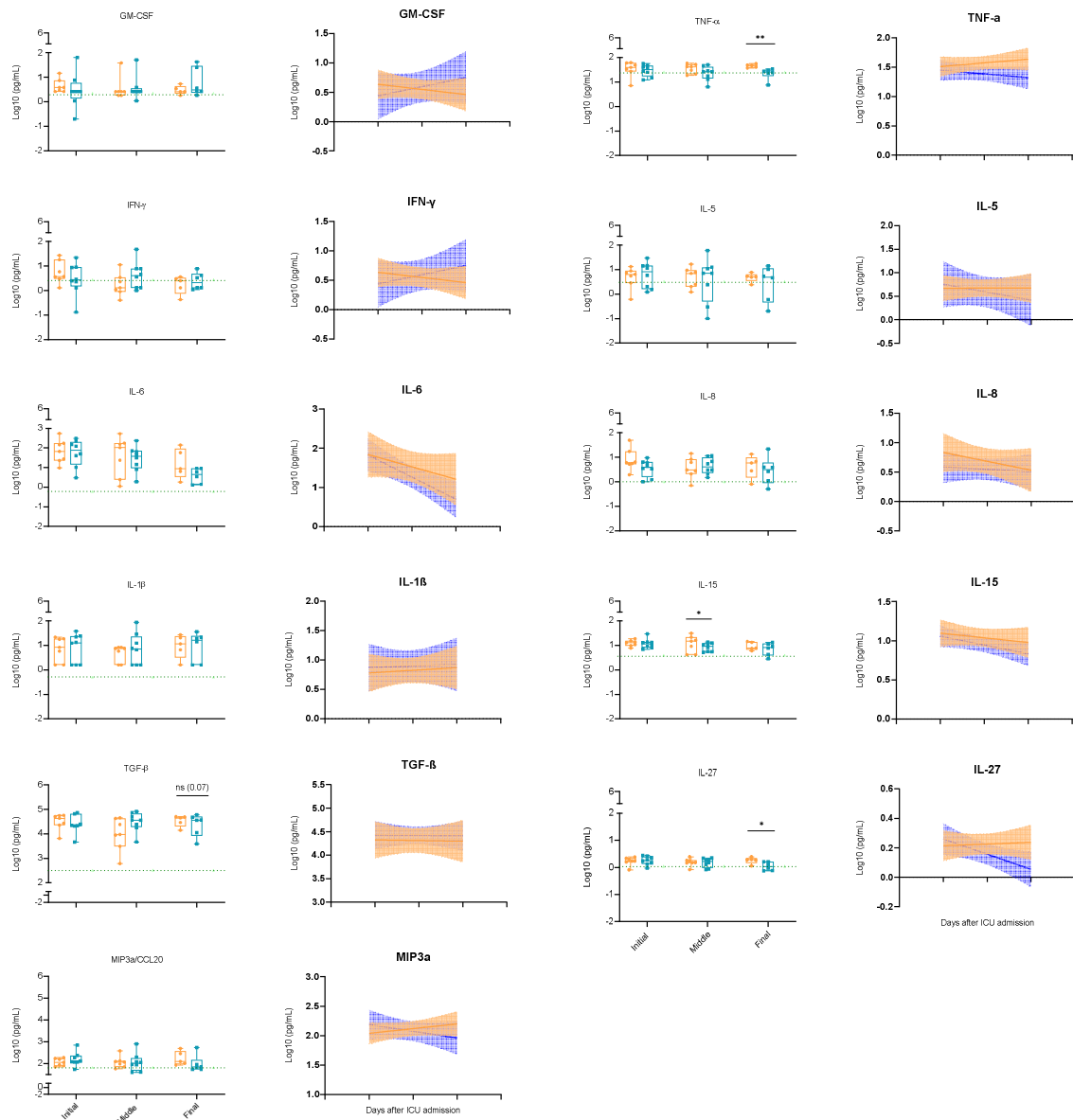


Figure 13| Longitudinal analysis of altered cytokine levels between severe and critical COVID-19 patients. Left, comparison of cytokines levels between severe (green) and critical (orange) COVID-19 patients at different times after UCI admission. The boxplots show medians (middle line) and third and first quartiles (boxes), while the whiskers show the minimum and maximum observed, each dot represents a patient. Right, regression lines indicate cytokines progression along ICU stay time in severe (purple) and critical (orange) ICU patients. Shading represents 95% confidence interval (CI). P values were determined with unpaired, two-sided Mann–Whitney U-test. (ns $p > 0.05$; * $p \leq 0.05$; ** $p \leq 0.01$)

CHAPTER IV: Discussion and Future Perspectives

1. Discussion

The COVID-19 pandemic, caused by SARS-CoV-2, has affected millions of people worldwide, inflaming an unprecedented effort from the scientific community to understand the biological processes underlying SARS-CoV-2 infection. In this thesis, we aimed to characterize the immune responses triggered by SARS-CoV-2 and also find patterns associated with the quality and amplitude of immune responses in a cohort of ICU COVID-19 patients.

Elderly age is known to be associated with a reduced immune response and increased prevalence of underlying comorbidities, which may explain the poor clinical states observed in the majority of these patients⁶¹. In agreement with previous reports⁶²⁻⁶⁴, in our study, 15 out of 17 patients (88%) were characterized by a severe clinical state of the disease and had more than 50 years old. Therefore, our data suggests an association between age and severity of the disease. Additionally, 76.5% of these patients were male, higher than those reported by other studies (59%, 60.3%, and 56,9%)⁶²⁻⁶⁴. COVID-19 patients showed a difference in the severity and fatality rates between males and females. This may be explained by different sex hormones such as estrogen and testosterone, which have different immunoregulatory functions and could influence immune response and disease severity⁶⁵. Furthermore, the Spike receptor, ACE2, is located on the X chromosome, and some studies suggest the possible existence of alleles that confer resistance to COVID-19¹.

Similar to those demonstrated in previous studies⁶²⁻⁶⁴, the most common symptoms included fever (88%), cough (70%), and dyspnoea (47%). Baseline comorbidities were frequent in 82% of patients involved in this study, which was superior to those reported by Zhang *et al.*^{62,64} (79.3%) and Zhou *et al.*⁶³ (78.2%). The most prominent risk factors among the cohort population were high blood pressure (64%), diabetes mellitus (53%), and obesity (18%), with increased percentages compared to those demonstrated in the abovementioned studies. The mortality of the 17 hospitalized cases in the present study was 12% (2 out of 17 patients), lower than reported by Zhang *et al.*^{62,64} (17.0%) and Zhou *et al.*⁶³ (28.3%), but greatly higher than reported by Guan *et. al*⁶⁶ (1.4%). The differences observed between studies may be due to the large variation between sample sizes and case inclusion.

CRP is an acute-phase protein of hepatic origin triggered by IL-6 secretion and is widely used as a clinical biomarker to monitor the inflammation status upon infection or an insult⁶⁷. Several studies demonstrated that CRP blood levels are correlated with COVID-19 disease severity, progression, and mortality, making it a good predictor for severe illness and possibly useful to stratify patients^{68,69}. In this study, the cohort was stratified according to CRP levels, *i.e.*, patients with CRP above 200 µg/mL were classified as critical while patients with CRP levels below or equal to 200 µg/mL were classified as severe. The threshold was defined based on the distribution of data points observed when

representing the CRP levels on admission for all patients. However, to higher accuracy, the threshold should be based on several other parameters, such as lymphopenia, low levels of haemoglobin, elevated levels of leukocytes, aspartate aminotransferase, alanine aminotransferase, blood creatinine, blood urea nitrogen, troponin, creatine kinase, IL-6, ferritin, lactate dehydrogenase, among others⁷⁰.

The median age was 55 years in patients with severe disease status, whereas for the critical subgroup was of 63 years. However the median age in non-survival patients was 83 years. This data supports the concept that elder patients are more prone to develop severe illness. On contrary, no significant differences in both groups were observed in male and female ratios. However, of note, all non-survival patients were male. As expected, patients with severe progression underwent a greater number of therapeutic regimens to prevent disease progression and eventually death. Furthermore, no significant associations were found between the remaining clinical parameters and stratified patients.

Regarding antibody responses, we did not find significant differences between severe and critical patient groups when analyzing spike S1-, S2-, and nucleocapsid-specific IgG and IgM antibodies during UCI stay time. In addition, we found that spike S1-specific IgM and IgG antibodies were much higher when compared to nucleocapsid-specific antibodies. Consistent with our observations, previous studies have also found that spike protein is more immunogenic than nucleocapsid, suggesting that anti-S1 antibodies play an important role in viral clearance and recovery of patients⁷¹⁻⁷⁵. Curiously, we did not find spike S2-specific IgG and IgM antibody responses suggesting a low immunogenicity of these subunit domain. Our observations showed that IgG antibody responses against spike S1 and nucleocapsid were already 4-fold and 2-fold increased relative to background., on early stage of hospitalization (on admission). Nonetheless, IgG antibody titers continued to increase until approximately day 6 after ICU admission, where it achieve a plateau (7-fold higher than background assay). In the case of IgM antibody response, they remained constant during ICU stay time. The Spike S1-specific IgM antibodies were maintained at a 2-fold increasing, and nucleocapsid-specific IgM was maintained close to the background. These kinetic profile of all tested antibodies are consistent with previous reports, however timeline variations in kinetic responses were observed among several studies⁷¹⁻⁷⁵. Regarding IgA antibodies is noteworthy that these antibodies are predominantly associated with the immune response in the mucosal membranes, being in small percentages in the plasma samples. In the case of spike S1- and nucleocapsid-specific IgA levels we observed a great variation between severe and critical patients. IgA antibody levels increased until reaching a peak around day 6 of ICU admission, followed by a rapid decline close to the cut-point value in both groups. However, the variation in the antibody responses was extremely disparate in critical patients (more than 8-fold). Previous reports are consistent with the observations in the current

study⁷⁵⁻⁷⁷. Interestingly, Sterlin *et. al*,⁷⁶ demonstrated that SARS-CoV-2 infection induces an early potent IgA immune response. Importantly, it was found that IgA antibodies purified from serum, were more effective in neutralizing the virus than IgG antibodies, suggesting that weak IgA antibody response in the early stage of infection may be associated with the disease progression. Nonetheless, it is important to note that the non-survival COVID-19 patients in this study failed to develop high titer antibodies against the several SARS-CoV-2 proteins tested (Spike S1,S2, and Nucleocapsid), consistent with a previous study that found antibody levels significantly lower in non-survivors than in survivors⁵⁰. Our results suggest that antibody responses against SARS-CoV-2 play an essential role in COVID-19 survival⁷⁸. Based on these observations, monitoring the dynamic changes of antibodies may provide important clinical information for diagnosis, and disease prognosis. In regard to antibody persistence, the lack of blood samples collected from patients after ICU discharge did not allow us to determine how long the antibody response could last.

In order to determine the association between the antibody levels and the disease status (severe and critical), we performed several correlations between antibody titers and CRP levels. A strong positive correlation was observed between S1 binding IgG antibody titers and CRP levels (both variables determined on admission) in the severe group. These results suggest that IgG levels increase as the disease becomes more severe. Furthermore, in the critical group it was observed moderate negative correlations between S1 binding IgG and IgA antibody titers versus CRP levels (both determined on admission), yet statistically not significant, probably due to the small sample size. Strikingly, we found a likely association between low levels of S1 binding IgG and IgA with worse disease outcomes.

Neutralizing antibodies (NAbs) have an important role in virus clearance and play a key function in immune protection or treatment against viral diseases such as COVID-19. Virus-specific NAbs, induced through either infection or vaccination, have the capacity to block viral infection⁷⁹. Recently, passive antibody therapy, such as plasma infusion from convalescent patients has led to a clear clinical improvement of both mild and severe COVID-19 patients. The efficacy observed have been associated with the concentration of antibodies more specifically NAbs in plasma of recovered donors⁸⁰. In this study we developed a surrogate virus neutralization assay to measure SARS-Cov-2-specific NAbs in plasma samples from ICU COVID-19 patients. The assay developed demonstrated high sensitivity and reproducibility (ROC-AUC 0.97 and Sp 95%, Se 89%, $p < 0.001$). We observed that on early stage of hospitalization, patients already presented low titers of neutralizing antibodies, however these titers were still relatively low ($IC_{50} = 10$). It is noteworthy that patients with severe clinical status showed a slight increase in Nab titers in relation to patients with critical status. The titers of NAbs reached their peak at day 6 after UCI admission and remained stable thereafter. Overall, and during hospitalization in intensive care unit, severe patients showed a neutralizing antibody kinetic

activity identical to critical patients but presented always a better Nab activity. Our results are consistent with previous studies, even though we had detected antibody titers later in time^{79,81}.

The NAb titers in the cohort were observed to be negatively correlated with both CRP groups. Thus, severe group presented a Spearman's coefficient of 0.76 ($p=0.08$) whereas critical patients presented a coefficient of approximately 0.6 ($p=0.096$). In addition, we also detected a strong association between variables, Nab titers versus S1-specific IgG antibody titers in critical patients ($r=0.6$; $p<0.0005$). For the IgA to IgG ratio antibody levels, the associations were weaker ranging between $r=0.26$ for low CRP and $r=0.4$ for critical patients, but significant in the severe group ($p=0.009$). These results are consistent with previous reports that demonstrated that IgG titers are highly correlated with Nabs titers, although other classes of antibodies can also play a role in virus neutralization^{54,82}.

Previous studies had demonstrated that the RBD-targeting neutralizing antibodies are immunodominant during SARS-CoV-2 infections⁸³. Nonetheless, within the diversity of epitopes in RBD, not all will have the same ability to produce antibody responses⁸⁴. Based on these observations, we decided to study the reactivity of COVID-19 patients' plasma samples against the SARS-CoV-2 RBD epitopes. Nineteen overlapping peptides have been designed to mimic RBD epitopes, and the antigenic response of each has been accessed by ELISA. Notably, we are only analyzing linear epitopes, conformational epitopes, also known as discontinuous epitopes, were not considered in this assay.

Our results demonstrated, for the first time, the existence of two clusters of peptides, here defined as cluster 1 and cluster 2, in which the reactivity of ICU patients' plasma samples was higher. These clusters were located at N- and C-terminal of the RBD domain, respectively. Notably, when comparing the reactivity among the two clusters it was possible to observe that Cluster 2 showed highly increased reactivity compared with cluster 1. It was also possible to observe that in cluster 2, stands out a peptide (Bio-NT-20) with increased reactivity compared to the remaining. Interestingly, when analyzing the cluster's location in SARS-CoV-2 spike three-dimensional structure, we see that cluster 2 is located in the RBD site of interaction with its receptor, the ACE2. Contrasting cluster 1, is located in the opposite location of the RBD-ACE2 site of interaction. Moreover, peptides with low immunoreactivity are located in an interior location in the RBD three-dimensional structure which may explain the low reactivity of ICU patients' plasma samples observed.

Previous studies identified 6 residues in RBD amino acid structure critical for binding to ACE2, these residues are L455, F486, Q493, S494, N501, and Y501⁸⁵. Curiously, these residues are located in cluster 2 suggesting that antibodies targeting these epitopes are more likely to be neutralizing antibodies.

Nonetheless, our results demonstrate that all ICU patients developed antibodies against the RBD epitopes. Further, when analyzing the response among the several stratification groups (severe and critical), we did not find significant differences in peptides immunoreactivity. However, it was possible to perceive that in both stratification groups, some patients, exhibited a distinct pattern of reactivity across RBD epitopes. Interpreting, the results obtained in non-survival patients we could not identify meaningful differences that could explain the outcome observed in these patients. These results suggest that patients' disease progression is not only associated with the target of the antibodies, but also with other immune responses, including T cells or cytokines.

In order to evaluate the longitudinal variation of antibody reactivity along, we analyzed plasma samples collected on admission, mid-, and end-hospitalization at ICU. Our data demonstrated that there was no variation in the reactive peptides. Cluster 1 and 2 continue to have higher reactivity compared with the remaining ones. However, it was possible to observe an increase in reactivity throughout time of hospitalization in almost all patients. These results are consistent with the expected considering the improvements observed in the clinical status of patients.

It is important to note, that we are analyzing a polyclonal sera samples and thus the high reactivity of samples to some peptides does not necessarily mean that these peptides are the most important to conceive protection. In fact, the most dominant epitopes do not necessarily correspond to the most effective ones⁸⁴. Further studies are needed to confirm the neutralizing ability of the antibodies targeting these two clusters. Since antibodies without neutralizing capability against the virus might enhance the cellular immune and inflammatory responses which result in a deregulated immune response that can be the causes of SARS-CoV-2 severe outcomes⁸⁴.

Surprisingly, a study that has been performed by an independent group in FFUL has demonstrated that the N-terminal of the RBD domain is the most variable region among the several SARS-CoV-2 specimens tested. Although it is also the place where the amino acid residues are essential to ACE2 binding. These results may also suggest that SARS-CoV-2 is trying to hide the most effective neutralizing epitopes, redirecting the response to epitopes with a lower protective capacity. Based on these observations, all epitope-based vaccines developed against this region must be carefully analyzed.

Elevated levels of inflammatory cytokines have been associated with poor outcomes among COVID-19 patients. Herein, we focus on the longitudinal analysis of several cytokines and chemokines in ICU patients with COVID-19 and try to find correlations between disease status and disease course. Herein we observed a COVID-19 signature characterized by an upregulation of several inflammatory cytokines and chemokines that was shared by both severe and critical disease groups of which we highlight the following: GM-CSF, TNF- α , IFN- γ , IL-1 β , IL-5, IL-6, IL-8, IL-15, IL-

27, and MIP3a. These data highlight broad inflammatory changes, involved with the innate and adaptive cell-mediated effector immunity⁸⁶. This analyse is strongly supported by previous observation, which demonstrate that both mild and severe forms of disease result in changes cytokine secretion, particularly such as IL-6, TNF, IL-1, IL-2, IL-17, IFN- γ , GM-CSF, MCP-1 (macrophage inflammatory protein 1), IP-10 (IFN- γ -induced protein 10), IL-17, MCP-3, IL-1ra, and others^{87,88}. Notably, in patients that had succumbed to COVID-19 (Y005 and Y014) we identified a divergent cytokine profile. In patient Y014, most of the cytokines as such TNF- β , IFN- γ , IL-4, IL-5, IL-6, IL-8, IL-9, IL-10, IL-12p70, IL-15, TGF- β , IL-27, IL-28a, and MIP3a were highly altered. Contrasting, a weak cytokine response was observed in patient Y005. Of note, IL-10 was extremely high in this patient. Previous reports demonstrated that a lack of negative feedback mechanisms by cytokines like IL-10 and IL-4 could increase the severity of cytokines response pathogenic CRS or cytokine storm⁸⁹. On the other hand, the excessive release of these anti-inflammatory cytokines may lead to a feeble response, as observed in patient Y005. As anticipated IL-6, IL-8 and MIP3a expression levels were significantly low in patients with moderate disease (Y006 and Y007). These finding are consistent with previous reports that showed plasma concentrations of these cytokines are associated with cytokine storm and are remarkable associated with disease severity^{90,91}. Although, we did not observe significant differences in the expression of inflammatory markers along disease progression between severe and critical patients, linear regression analysis showed increase levels TNF- α , IL-6, IL-27, and MIP3a in patients with critical disease but declined in patients with severe disease. Furthermore, the remaining cytokines tended to decline steadily over time, approaching the levels of healthy individuals, at the time of discharge. These results are consistent with the findings reported by Lucas et. al. ⁸⁷, that demonstrated that patients underlying a critical disease status have tendency to increase or stabilize pro-inflammatory cytokine levels along time, where patients with moderate disease normally decrease cytokine levels to levels close to baseline.

Finally, is important to note that this study has some limitations. First, the sample size was very small, not allowing the study to be robust. Second, this study lacks a moderate group of patients. The existence of this group would allow finding discriminatory markers involved in disease progression and clinical evolution. Finally, there is a paucity of clinical information that would allow categorizing patients more rigorously.

2. Conclusion and Future Perspectives

In conclusion, several mechanisms of host immune response are being implicated in COVID-19 immunopathogenesis. Measuring antibody responses during disease may contribute for estimate which patients most likely develop severe clinical outcomes. Furthermore, the cytokine signature responses may give important hints to clinicians to modulate the inflammatory immune response in early disease stage avoiding bad clinical trajectories and deaths. However, further studies are needed to better understand these mechanisms, since they will provide vital information for the treatment and management of the disease, including for the development of new effective therapies.

REFERENCES

1. Tay, M. Z., Poh, C. M., Rénia, L., Macary, P. A. & Ng, L. F. P. The trinity of COVID-19: immunity, inflammation and intervention. *Nat. Rev. Immunol.* **20**, 363–374 (2020).
2. WHO Coronavirus Disease (COVID-19) events as they happen. Available online: <https://www.who.int/emergencies/diseases/novel-coronavirus-2019/events-as-they-happen>.
3. WHO Coronavirus Disease (COVID-19) Dashbord. Available online: <https://covid19.who.int/>.
4. Organization, W. H. Transmission of SARS-CoV-2: implications for infection prevention precautions. (2020).
5. Fung, T. S. & Liu, D. X. Human Coronavirus: Host-Pathogen Interaction. *Annu. Rev. of Microbiology* 529–556 (2019).
6. Anderson, K. G., Rambaut, A., Limkin, W. I., Holmes, E. C. & Garry, R. F. The proximal origin of SARS-CoV-2. *Nat. Med.* **26**, 450–452 (2020).
7. Lu, R. *et al.* Genomic characterisation and epidemiology of 2019 novel coronavirus: implications for virus origins and receptor binding. *Lancet* **395**, 565–574 (2020).
8. Zhou, P. *et al.* A pneumonia outbreak associated with a new coronavirus of probable bat origin. *Nature* **579**, (2020).
9. Tao, Z. *et al.* A new coronavirus associated with human respiratory disease in China. *Nature* **579**, 265–269 (2020).
10. Paraskevisa, D. *et al.* Full-genome evolutionary analysis of the novel corona virus (2019-nCoV) rejects the hypothesis of emergence as a result of a recent recombination event. *Elsevier* **79**, 1567–1348 (2020).
11. Xiao, K. *et al.* Isolation of SARS-CoV-2-related coronavirus from Malayan pangolins. *Nature* **583**, 286–289 (2020).
12. Hu, B. Characteristics of SARS-CoV-2 and COVID-19. *Nat. Rev. Microbiol.* (2019). doi:10.1038/s41579-020-00459-7
13. Shah, V. K., Firmal, P., Alam, A. & Ganguly, D. Overview of Immune Response During SARS-CoV-2 Infection: Lessons From the Past. **11**, 1–17 (2020).
14. Astuti, I. Severe Acute Respiratory Syndrome Coronavirus 2 (SARS-CoV-2): An overview of viral structure and host response. *Diabetes Metab. Syndr. Clin. Res. Rev.* **14**, 407–412 (2020).
15. Li, F. Structure, Function, and Evolution of Coronavirus Spike Proteins. 237–264 (2016). doi:10.1146/annurev-virology-110615-042301
16. Clausen, T. M. *et al.* SARS-CoV-2 Infection Depends on Cellular Heparan Sulfate and ACE2. *Cell* **183**, 1043-1057.e15 (2020).
17. Shang, J. *et al.* Cell entry mechanisms of SARS-CoV-2. *PNAS* **117**, 11727–11734 (2020).
18. Hoffmann, M. *et al.* SARS-CoV-2 Cell Entry Depends on ACE2 and TMPRSS2 and Is Blocked by a Clinically Proven Protease Inhibitor. *Cell* **181**, 271–280 (2020).
19. Harapan, H. *et al.* Coronavirus disease 2019 (COVID-19): A literature review. *J. Infect. Public Health* **13**, 667–673 (2020).
20. Feng, J. *et al.* Clinical characteristics of 82 death cases with COVID-19. *medRxiv* (2020).
21. Gupta, A. *et al.* Extrapulmonary manifestations of COVID-19. *Nat. Med.* **26**, 1017–1032 (2020).
22. Wu, Y. *et al.* Correspondence Prolonged presence of SARS-CoV-2 viral RNA in faecal samples. *Lancet Gastroenterol. Hepatol.* **5**, 434–435 (2020).

23. Wang, W. *et al.* Detection of SARS-CoV-2 in Different Types of Clinical Specimens. *JAMA* **323**, (2020).
24. World Health Organization. Diagnostic testing for SARS-CoV-2. *World Heal. Organ.* 1–20 (2020).
25. Liu, R. *et al.* Positive rate of RT-PCR detection of SARS-CoV-2 infection in 4880 cases from one hospital in Wuhan, China, from Jan to Feb 2020. *Clin. Chim. Acta.* **505**, 172–175 (2020).
26. Winichakoon, P. *et al.* Negative Nasopharyngeal and Oropharyngeal Swabs Do Not Rule Out COVID-19. *J. Clin. Microbiol.* **58**, 297–320 (2020).
27. Chen, W. *et al.* Detectable 2019-nCoV viral RNA in blood is a strong indicator for the further clinical severity. *Emerging microbes & infections* **9**, 469–473 (2020).
28. Wong, M. C. *et al.* Detection of SARS-CoV-2 RNA in fecal specimens of patients with confirmed COVID-19: A meta-analysis. *J. Infect.* **81**, e31–e38 (2020).
29. Amanat, F. *et al.* A serological assay to detect SARS-CoV-2 seroconversion in humans. *Nat. Med.* **26**, 1033–1036 (2020).
30. COVID-19 Vaccine Tracker. Available online: <https://biorender.com/covid-vaccine-tracker>.
31. How the body reacts to viruses. Available online: <https://onlinelearning.hms.harvard.edu/hmx/immunity/>.
32. Abbas, A., Lichtman, A. & Pillai, S. *Cellular and Molecular Immunology*. (2012).
33. Innate Immunity Overview. Available online: <https://www.khanacademy.org/test-prep/mcat/organ-systems/the-immune-system/a/innate-immunity>.
34. Vabret, N. *et al.* Immunology of COVID-19: Current State of the Science Nicolas. (2020).
35. Hadjadj, J., Yatim, N., Barnabei, L., Corneau, A. & Boussier, J. Impaired type I interferon activity and inflammatory responses in severe COVID-19 patients. **724**, 718–724 (2020).
36. Prokunina-olsson, L. COVID-19 and emerging viral infections : The case for interferon lambda. *J. Exp. Med.* **217**, 5–8 (2020).
37. Huang, C. *et al.* Clinical features of patients infected with 2019 novel coronavirus in Wuhan, China. *Lancet* **395**, 497–506 (2020).
38. Mehta, P. *et al.* COVID-19: consider cytokine storm syndromes and immunosuppression. *Lancet* **395**, 1033–1034 (2020).
39. Wang, F. *et al.* Characteristics of Peripheral Lymphocyte Subset Alteration in COVID-19 Pneumonia. *J. Infect. Dis.* (2020). doi:10.1093/infdis/jiaa150
40. Yu, L., Tong, Y., Shen, G. & Fu, A. Immunodepletion with Hypoxemia : A Potential High Risk Subtype of Coronavirus Disease 2019. *medRxiv* (2020).
41. Zheng, H. *et al.* Elevated exhaustion levels and reduced functional diversity of T cells in peripheral blood may predict severe progression in COVID-19 patients. *Cell. Mol. Immunol.* 17–19 (2020). doi:10.1038/s41423-020-0401-3
42. Kim, J. *et al.* Innate immune crosstalk in asthmatic airways : Innate lymphoid cells coordinate polarization of lung macrophages. *J. Allergy Clin. Immunol.* (2018). doi:10.1016/j.jaci.2018.10.040
43. Chen, G. *et al.* Clinical and immunological features of severe and moderate coronavirus disease 2019 Clinical and immunological features of severe and moderate coronavirus disease 2019. *J. Clin. Invest.* **130**, 2620–2629 (2020).

44. Nie, S. *et al.* Metabolic disturbances and inflammatory dysfunction predict severity of coronavirus disease 2019 (COVID-19): a retrospective study . *medRxiv* (2020).
45. Qiang Zeng, M. *et al.* Mortality of COVID-19 is Associated with Cellular Immune Function Compared to Immune Function in Chinese Han Population. *medRxiv* (2020).
46. Wu, Y. & Chen, Y. Reduction and Functional Exhaustion of T Cells in Patients With Coronavirus Disease 2019. *Front. Immunol.* **11**, (2020).
47. Xu, Z. *et al.* Pathological findings of COVID-19 associated with acute respiratory distress syndrome. *Lancet Respir.* **2600**, 19–21 (2020).
48. Qin, C. *et al.* Dysregulation of Immune Response in Patients With Coronavirus 2019 (COVID-19) in Wuhan, China. *Clin. Infect. Dis.* **2019**, 4–10 (2020).
49. Zhou, Y. *et al.* Pathogenic T-cells and inflammatory monocytes incite inflammatory storms in severe COVID-19 patients. *Natl. Sci. Rev.* **7**, 998–1002 (2020).
50. Li, K. *et al.* Dynamic changes in anti-SARS-CoV-2 antibodies during SARS-CoV-2 infection and recovery from COVID-19. (2020). doi:10.1038/s41467-020-19943-y
51. Thevarajan, I. *et al.* Breadth of concomitant immune responses prior to patient recovery : a case report of non-severe COVID-19. *Nat. Med.* **26**, 450–455 (2020).
52. Wu, H.-S. *et al.* Early Detection of Antibodies against Various Structural Proteins of the SARS-Associated Coronavirus in SARS Patients. *J. Biomed. Sci.* **11**, 117–126 (2004).
53. Nie, Y. *et al.* Neutralizing Antibodies in Patients with Severe Acute Respiratory Syndrome – Associated Coronavirus Infection. *J. Infect. Dis.* **190**, 1119–1126 (2004).
54. Jiang, S., Hillyer, C. & Du, L. Neutralizing Antibodies against SARS-CoV-2 and Other Human Coronaviruses. *Trends Immunol.* (2020). doi:10.1016/j.it.2020.03.007
55. Zhu, Z. *et al.* Potent cross-reactive neutralization of SARS coronavirus isolates by human monoclonal antibodies. *PNAS* **104**, 12123–12128 (2007).
56. Berry, J. D. *et al.* Neutralizing epitopes of the SARS-CoV S-protein cluster independent of repertoire , antigen structure or mAb technology. *Landes Biosci.* **2**, 53–66 (2010).
57. Liu, L. *et al.* Anti–spike IgG causes severe acute lung injury by skewing macrophage responses during acute SARS-CoV infection. *J. Clin. Immunol. Insight* **4**, 1–19 (2019).
58. Zhang, L. *et al.* Antibody Responses Against SARS Coronavirus Are Correlated With Disease Outcome of Infected Individuals. *J. Med. Virol.* **78**, 1–8 (2006).
59. Metsalu, T., Vilo, J., Science, C. & Liivi, J. ClustVis : a web tool for visualizing clustering of multivariate data using Principal Component Analysis and heatmap. *Nucleic Acids Res.* **43**, 566–570 (2015).
60. Tan, C. W. *et al.* A SARS-CoV-2 surrogate virus neutralization test based on antibody-mediated blockage of ACE2–spike protein–protein interaction. *Nat. Biotechnol.* doi:10.1038/s41587-020-0631-z
61. Opal, S. M., Girard, T. D. & Ely, E. W. The Immunopathogenesis of Sepsis in Elderly Patients. **41**, 504–512 (2005).
62. Cao, J. Z. Y. *et al.* Clinical, radiological, and laboratory characteristics and risk factors for severity and mortality of 289 hospitalized COVID-19 patients. (2020). doi:10.1111/all.14496
63. Zhou, F. *et al.* Clinical course and risk factors for mortality of adult inpatients with COVID-19 in Wuhan , China : a retrospective cohort study. *Lancet* **395**, 1054–1062 (2020).

64. Xiang, J. Z., Cao, D. Y., Yang, Y. Y. Y., Cezmi, Y. Y. & Gao, A. A. Y. Clinical characteristics of 140 patients infected with SARS-CoV-2 in Wuhan , China. 1730–1741 (2020). doi:10.1111/all.14238
65. Taneja, V. Sex Hormones Determine Immune Response. *Front. Immunol.* **9**, (2018).
66. Guan, W. *et al.* Clinical Characteristics of Coronavirus Disease 2019 in China. (2020). doi:10.1056/NEJMoa2002032
67. Thompson, D., Pepys, M. B. & Wood, S. P. The physiological structure of human C-reactive protein and its complex with phosphocholine. *Elsevier Sci.* **1999**, 169–177
68. Microbiol, C. *et al.* Plasma CRP level is positively associated with the severity of COVID - 19. *Ann. Clin. Microbiol. Antimicrob.* (2020). doi:10.1186/s12941-020-00362-2
69. Wang, L. C-reactive protein levels in the early stage of COVID-19. *Med. Mal. Infect.* **50**, 332–334 (2020).
70. Mudatsir, M. *et al.* Predictors of COVID-19 severity : a systematic review and meta-analysis. **9**, 1–24 (2020).
71. Long, Q. *et al.* Antibody responses to SARS-CoV-2 in patients with COVID-19. *Nat. Med.* (2020). doi:10.1038/s41591-020-0897-1
72. Gazumyan, A. *et al.* Convergent antibody responses to SARS-CoV-2 in convalescent individuals. *Nature* (2020). doi:10.1038/s41586-020-2456-9
73. Sun, B. *et al.* Kinetics of SARS-CoV-2 specific IgM and IgG responses in COVID-19 patients. *Emerg. Microbes Infect.* **9**, 940–948 (2020).
74. Zhao, J. *et al.* Antibody Responses to SARS-CoV-2 in Patients With Novel Coronavirus Disease 2019. *Clin. Infect. Dis.* **71**, (2020).
75. Ma, H. *et al.* Serum IgA, IgM, and IgG responses in COVID-19. *Cell. Mol. Immunol.* 18–20 (2020). doi:10.1038/s41423-020-0474-z
76. Sterlin, A. D. & Mathian, A. IgA dominates the early neutralizing antibody response to SARS-CoV-2. *medRxiv* 25–28 (2020).
77. Padoan, A. *et al.* Clinica Chimica Acta IgA-Ab response to spike glycoprotein of SARS-CoV-2 in patients with COVID-19 : A longitudinal study. *Clin. Chim. Acta* **507**, 164–166 (2020).
78. Secchi, M. *et al.* COVID-19 survival associates with the immunoglobulin response to the SARS-CoV-2 spike receptor binding domain. *J. Clin. Immunol.* **130**, 6366–6378 (2020).
79. Xun, J. *et al.* Neutralizing antibody responses to SARS-CoV-2 in a COVID-19 recovered patient cohort and their implications. (2020).
80. Chen, L., Xiong, J., Bao, L. & Shi, Y. Convalescent plasma as a potential therapy for COVID-19. *Lancet Infect. Dis.* **2**, 19–20 (2020).
81. Qin, C. & Jin, R. Potent Neutralizing Antibodies against SARS-CoV-2 Identified by High-Throughput Single-Cell Sequencing of Convalescent Patients' B Cells. *Cell* **182**, 73–84 (2020).
82. Liu, L. *et al.* Potent neutralizing antibodies directed to multiple epitopes on SARS-CoV-2 spike. *Nature* (2020). doi:10.1038/s41586-020-2571-7
83. Premkumar, L. *et al.* The receptor-binding domain of the viral spike protein is an immunodominant and highly specific target of antibodies in SARS-CoV-2 patients. *Sci. Immunol.* (2019).
84. Gershoni, J. M., Roitburd-berman, A., Siman-tov, D. D. & Freund, N. T. Epitope Mapping The

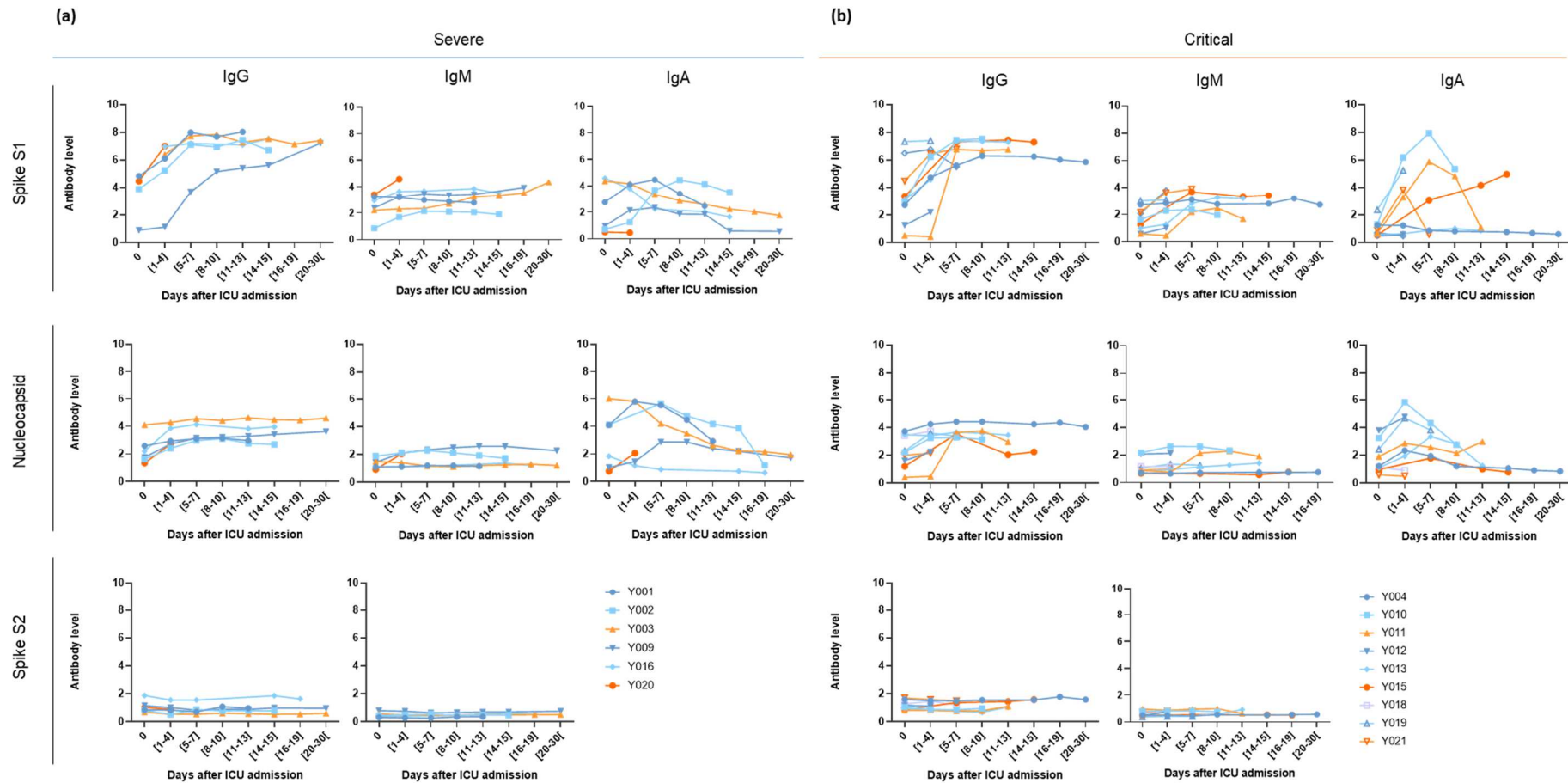
First Step in Developing Epitope-Based Vaccines. *Elsevier* **21**, 145–156 (2007).

85. Wan, Y., Shang, J., Graham, R., Baric, R. S. & Li, F. Receptor Recognition by the Novel Coronavirus from Wuhan : an Analysis Based on Decade-Long Structural Studies of SARS Coronavirus. *J. Virol.* **94**, 127–136 (2020).
86. Annunziato, F., Romagnani, C. & Romagnani, S. The 3 major types of innate and adaptive cell-mediated effector immunity. *J. Allergy Clin. Immunol.* **135**, 626–635
87. Lucas, C. *et al.* Longitudinal analyses reveal immunological misfiring in severe COVID-19. *Nature* **584**, 463–483 (2020).
88. Storm, C., Nowill, A. E. & Campos-lima, P. O. De. Immune Response Resetting as a Novel Strategy to Overcome SARS-CoV-2 – Induced Cytokine Storm. *J. Immunol.* **205**, 2566–2575 (2020).
89. Tisoncik, J. R. *et al.* Into the Eye of the Cytokine Storm. *Microbiol. Mol. Biol. Rev.* **76**, 16–32 (2012).
90. Zho, Z. *et al.* Heightened Innate Immune Responses in the Respiratory Tract of COVID-19 Patients. *Cell Host Microbe* **27**, 883–890 (2020).
91. Netea, M. G. *et al.* Complex Immune Dysregulation in COVID-19 Patients with Severe Respiratory Failure. *Cell Host Microbe* **27**, 992-1000.e3 (2020).

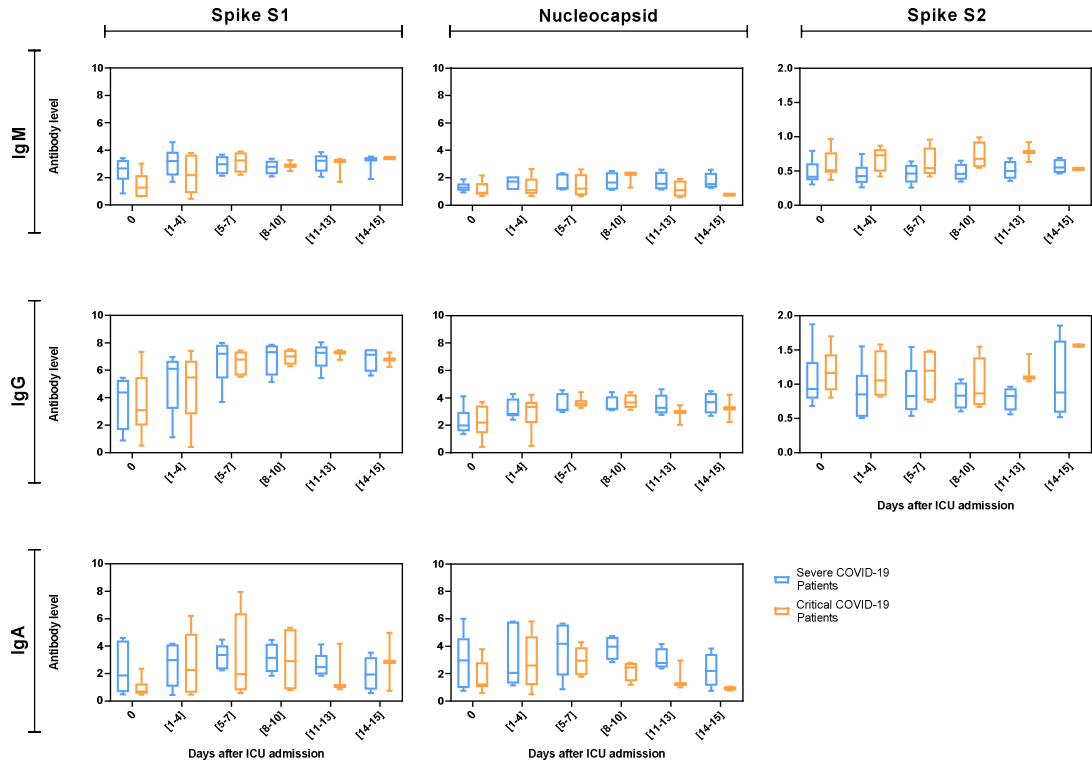
ANNEXES

10	20	30	40	50	
	MFVFLVLLPL	VSSQCVNLTT	RTQLPPAYTN	SFTRGVYYPD	KVFRSSVLHS
	60	70	80	90	100
	TQDLFLPFFS	NVTWFHAIHV	SGTNGTKRFD	NPVLPFNDGV	YFASTEKSNI
	110	120	130	140	150
	IRGWIFGTTL	DSKTQSLLV	NNATNVVIKV	CEFQFCNDPF	LGVYYHKNNK
	160	170	180	190	200
	SWMESEFRVY	SSANNCTFEY	VSQPFLMDLE	GKQGNFKNLR	EFVFKNIDGY
	210	220	230	240	250
	FKIYSKHTPI	NLVRDLPQGF	SALEPLVDLP	IGINITRFQT	LLALHRSYLT
	260	270	280	290	300
	PGDSSSGWTA	GAAAYYVGYL	QPRTFLLKYN	ENGTITDAVD	CALDPLSETK
	310	320	330	340	350
	CTLKSFTVEK	GIYQTSNFRV	OPTESIVRFP	<u>NITNLCPFGE</u>	<u>VFNATRFASV</u>
	360	370	380	390	400
	<u>YAWNRKRISN</u>	<u>CVADYSVLYN</u>	<u>SASFSTFKCY</u>	<u>GVSPTKLNDL</u>	<u>CFTNVYADSF</u>
	410	420	430	440	450
	<u>VIRGDEVROI</u>	<u>APGQTGKIAD</u>	<u>YNYKLPDDFT</u>	<u>GCVIAWNSNN</u>	<u>LDSKVGGNYN</u>
	460	470	480	490	500
	<u>YLYRLFRKSN</u>	<u>LKPFERDIST</u>	<u>EIYQAGSTPC</u>	<u>NGVEGFNCYF</u>	<u>PLQSYGFQPT</u>
	510	520	530	540	550
	<u>NGVGYQPYRV</u>	<u>VVLSFELLHA</u>	<u>PATVCGPKKS</u>	<u>TNLVKNKCVN</u>	<u>FNFNGLTGTG</u>
	560	570	580	590	600
	VLTESNKKFL	PFQQFGRDIA	DTTDAVRDPQ	TLEILDITPC	SFGGVSVITP
	610	620	630	640	650
	GTNTSNQVAV	LYQDVNCTEV	PVAIHADQLT	PTWRVYSTGS	NVFQTRAGCL
	660	670	680	690	700
	IGAHEVNNSY	ECDIPIGAGI	CASYQTQTN	PRRARSVASQ	SIIAYTMSLG
	710	720	730	740	750
	AENSVAYSNN	SIAIPTNFTI	SVTTEILPVS	MTKTSVDCTM	YICGDSTEC
	760	770	780	790	800
	NLLLQYGSFC	TQLNRALTGI	AVEQDKNTQE	VFAQVKQIYK	TPPIKDFGGF
	810	820	830	840	850
	NFSQILPDPS	KPSKRSFIED	LLFNKVTLAD	AGFIKQYGDC	LGDIAARDLI
	860	870	880	890	900
	CAQKFNGLTV	LPPLLTDEMI	AQYTSALLAG	TITSGWTFGA	GAALQIPFAM
	910	920	930	940	950
	QMAYRFNGIG	VTQNVLYENQ	KLIANQFNSA	IGKIQDSLSS	TASALGKLQD
	960	970	980	990	1000
	VVNQNAQALN	TLVKQLSSNF	GAISSVLNDI	LSRLDKVEAE	VQIDRLITGR
	1010	1020	1030	1040	1050
	LQSLQTYVTQ	QLIRAAEIRA	SANLAATKMS	ECVLGQSKRV	DFCGKGYHLM
	1060	1070	1080	1090	1100
	SFPQSAPHGV	VFLHVTYVPA	QEKNFITAPA	ICHDGKAHFP	REGVFSNGT
	1110	1120	1130	1140	1150
	HWFVTQRNFY	EPQIITDNT	FVSGNCDVVI	GIVNNTVYDP	LQPELDSFKE
	1160	1170	1180	1190	1200
	ELDKYFKNHT	SPDVDLGDIS	GINASVVNIQ	KEIDRLNEVA	KNLNESLIDL
	1210	1220	1230	1240	1250
	QELGKYEQYI	KWPWYIWLGF	IAGLIAIVMV	TIMLCCMTSC	CSCLKGCCSC
	1260	1270			
	GSCCKFDEDD	SEPVKGVKLV	HYT		

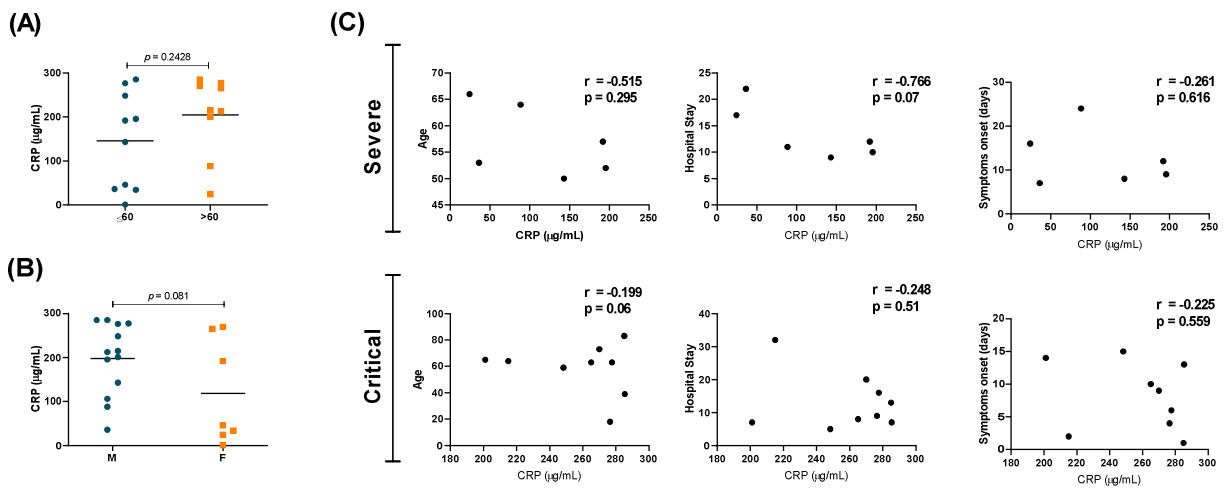
Extended Data Figure 1 | Sequence of the spike protein. S1 domain is shown in blue and orange (RBD). S2 domain is shown in green. In underlined is shown the amino acid sequence used to generate the peptide library.



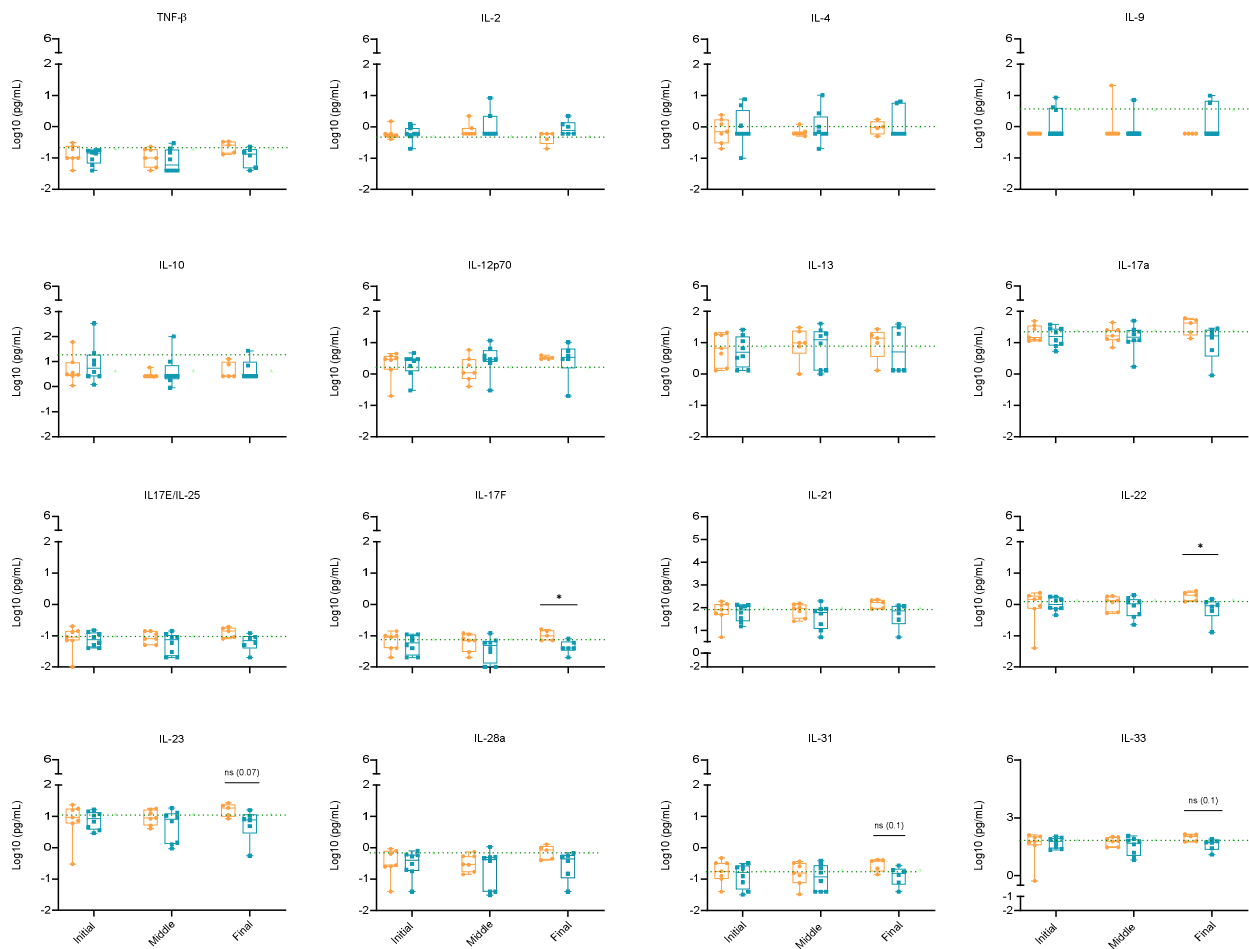
Extended Data Figure 2 | Antibody responses against SARS-CoV-2. Specific IgG, IgM, and IgA against SARS-CoV-2 spike S1, nucleocapsid and spike S2 were measured in severe (a) and critical COVID-19 patients (b) at different times after ICU admission. Antibody levels were presented as the absorbance 450nm divided by the cut point. (absorbance/cut point - Abs/CP) : S/CP > 1 was defined as positive and Abs/CP ≤ 1 as negative.



Extended Data Figure 3| Antibody responses against different SARS-CoV-2 antigens. Comparison of the different classes of antibodies between critical and severe COVID-19 patients at different time points after ICU admission. The boxplots show medians (middle line) and third and first quartiles (boxes), while the whiskers show the minimum and maximum observed. P values were determined with unpaired, two-sided Mann–Whitney U-test. No significant P values were obtained between the two groups.



Extended Data Figure 4| Association between CRP levels and clinical characteristics of the COVID-19 patients. (A) No significant difference in the CRP levels at the plateau was found between ≤ 60 y group (N = 10) and > 60 y group (N = 9) and **(B)** patients gender. Unpaired, two-sided Mann-Whitney U test was performed. **(C)** No association was found between the CRP levels at age, hospital stay and date from symptoms onset until ICU admission. Pearson correlation coefficients (r) and p value are depicted in plots.



Extended Data Figure 5 | Longitudinal analysis of cytokine levels between severe and critical COVID-19 patients. Comparison of cytokines levels between severe (green) and critical (orange) COVID-19 patients at different times after UCI admission. The boxplots show medians (middle line) and third and first quartiles (boxes), while the whiskers show the minimum and maximum observed, each dot represents a patient. P values were determined with unpaired, two-sided Mann-Whitney U-test. (ns $p > 0.05$; ** $p \leq 0.01$; * $p \leq 0.05$; *** $p \leq 0.001$; **** $p \leq 0.0001$)

Extended Data Table 1 | Cohort demographics and clinical characteristics.

Patient ID	Y001	Y002	Y003	Y004	Y005	Y009	Y010	Y011	Y012	Y013	Y014	Y015	Y016	Y018	Y019	Y020	Y021	TOTAL	CRP ≤200µg/mL	CRP >200µg/mL
Date of ICU admission (year/month/day)	14/04/2020	11/04/2020	15/04/2020	19/04/2020	20/04/2020	28/04/2020	30/04/2020	05/05/2020	10/05/2020	12/05/2020	13/05/2020	14/05/2020	14/05/2020	06/06/2020	08/06/2020	12/06/2020	14/06/2020			
Date of discharge (year/month/day)	23/04/2020	22/04/2020	27/04/2020	05/05/2020	22/04/2020	20/05/2020	07/05/2020	10/05/2020	23/05/2020	01/06/2020	22/05/2020	15/06/2020	01/06/2020	13/06/2020	16/06/2020	22/06/2020	23/06/2020			
Intensive care stay time (days)	9	11	12	16	2	22	7	5	13	20	9	32	17	7	8	10	9	12	14	13
Age (years)	50	64	57	63	83	53	39	59	83	73	83	64	66	65	63	52	18	61	57	59
Sex																				
Male	x	x		x	x	x	x	x	x		x	x		x		x	x	76.5% (13/17)	67% (4/6)	78% (7/9)
Female			x							x			x		x			23.5% (4/17)	33% (2/6)	22% (2/9)
COVID Risk factors																				
None	-	-	-	-	-	-	x	-	-	-	x	-	-	-	-	-	x	18% (3/17)	0% (0/6)	22% (2/9)
Cancer treatment	-	-	-	-	-	-	-	-	x (Leukemia)	-	-	-	-	-	-	-	-	6% (1/17)	0% (0/6)	11% (1/9)
Chronic Heart disease	-	-	-	-	-	-	-	-	-	-	-	-	x	-	-	-	-	6% (1/17)	17% (1/6)	0% (0/9)
Chronic Lung Disease	-	-	-	-	-	-	-	-	-	-	-	-	x	x	-	-	-	12% (2/17)	17% (1/6)	11% (1/9)
Chronic Renal Disease	-	-	-	-	x	-	-	-	x (Dialysis)	-	-	-	-	-	-	-	-	6% (1/17)	0% (0/6)	11% (1/9)
Solid organ transplant	-	-	-	-	-	-	-	-	-	-	-	-	-	-	-	-	-	0% (0/17)	0% (0/6)	0% (0/9)
HIV (with anti-viral treatment; CD4>400)	-	-	-	-	-	-	-	-	-	-	-	-	-	-	-	-	-	0% (0/17)	0% (0/6)	0% (0/9)
Diabetes	x	x	x	x	-	-	-	x	x	-	-	x	x	-	-	-	-	53% (8/17)	67% (4/6)	44% (4/9)
HTA	-	x	x	x	x	-	-	x	x	x	-	x	x	-	x	x	-	64% (11/17)	67% (4/6)	67% (6/9)
Obesity	-	-	x	-	-	-	-	-	-	-	-	-	x	-	-	x	-	18% (3/17)	50% (3/6)	0% (0/9)
Stroke	-	-	-	-	-	-	-	-	-	-	-	x	-	-	-	-	-	6% (1/17)	0% (0/6)	11% (1/9)
Other	-	-	-	-	-	x	-	-	-	-	-	-	-	-	x	-	-	12% (2/17)	17% (1/6)	11% (1/9)
Presenting Symptoms																				
Date from symptoms onset (days)	8	24	12	6	16	7	13	15	1	9	33	2	16	14	10	9	4	14	13	8
Headache	-	-	-	x	-	-	-	-	-	-	-	-	-	-	-	-	-	6% (1/17)	0% (0/6)	11% (1/9)
Objective fever (>37.9 °C)	-	x	x	x	-	x	x	x	x	x	x	x	x	x	x	x	x	88% (15/17)	83% (5/6)	100% (9/9)
Cough	x	x	x	x	x	-	x	x	x	x	x	-	x	x	-	-	-	70% (12/17)	67% (4/6)	67% (6/9)
Dyspnea	x	x	x	-	-	-	-	x	x	-	-	-	x	x	-	-	-	47% (8/17)	67% (4/6)	33% (3/9)
Rhinorrhea	-	-	-	-	-	-	-	-	-	-	-	-	-	-	-	-	-	0% (0/17)	0% (0/6)	0% (0/9)
Sore throat	-	-	-	-	-	-	-	-	-	-	-	-	-	-	x	-	-	6% (1/17)	0% (0/6)	11% (1/9)
Nausea	-	-	-	-	-	-	-	-	-	-	x	x	-	-	-	-	-	12% (2/17)	0% (0/6)	11% (1/9)
Vomiting	-	-	-	-	-	-	-	-	-	x	x	x	-	-	-	-	-	23% (4/17)	0% (0/6)	33% (3/9)
Diarrhea	x	-	-	-	-	-	-	-	-	-	-	-	-	x	-	-	-	23% (4/17)	17% (1/6)	22% (2/9)
Abdominal pain	-	-	-	-	-	-	-	x	-	-	-	-	-	-	-	-	-	12% (2/17)	0% (0/6)	22% (2/9)
Hypogeusia	-	-	-	-	-	-	-	-	x	-	-	-	-	-	-	-	-	12% (2/17)	17% (1/6)	11% (1/9)
Anosmia	-	-	-	-	-	-	-	-	-	-	-	-	-	-	-	x	-	6% (1/17)	17% (1/6)	0% (0/9)
Inflammatory markers																				
CRP µg/mL																				
First timepoint	143	88.4	192	277.6	106.4	36.2	285.4	248.3	285	270	212.7	215	24.3	201.1	265.1	195.6	276.5			
Middle timepoint	138	106.6	132	18.2	118.1	36.4	39.2	210.4	154.7	56.4	66.2	229.2	47.7	219.7	36.5	116.8	183.7			
Last timepoint	35.5	6.6	26.4	1.9	102.8	28.7	21.5	140.6	75.3	14.7	273.5	48.2	29.1	132.7	86	21	42			
Therapeutic drugs																				
Tocilizumab	-	x	-	x	-	-	-	-	-	-	-	-	-	-	-	-	-	12% (2/17)	17% (1/6)	11% (1/9)
Corticosteroids	-	-	x	-	-	-	-	x	-	x	-	-	x	-	x	-	x	41% (7/17)	33% (2/6)	44% (4/9)
Vasopressors	-	x	-	x	x	x	x	x	x	-	x	x	-	x	x	x	x	76% (17/17)	50% (3/6)	89% (8/9)
Other	-	-	-	-	-	-	Remdesivir	Remdesivir	-	-	-	Remdesivir	Remdesivir	Remdesivir	Remdesivir	Remdesivir	MIS-C (Fez/Mg)	47% (8/17)	33% (2/6)	67% (6/9)
Deceased																				
	-	-	-	-	x	-	-	-	-	-	x	-	-	-	-	-	-	12% (2/17)	Excluded	Excluded

Extended Data Table 2 | Amino acid sequence of the synthesized peptides and their location in the spike sequence.

PEPTIDE	POSITION(S) IN SPIKE SEQUENCE	AMINO ACID SEQUENCE
Bio-NV-20	(331-350)	NITNLCPFGGEVFNATRFASV
Bio-VN-20	(341-360)	VFNATRFASVYAWNRKRISN
Bio-YN-20	(351-370)	YAWNRKRISNCSVADYSVLYN
Bio-CY-20	(361-380)	CVADYSVLYNSASFSTFKCY
Bio-SL-20	(371-390)	SASFSTFKCYGVSPTKLNDL
Bio-GF-20	(381-400)	GVSPTKLNDLCFTNVYADSF
Bio-CF-20	(391-410)	CFTNVYADSFVIRGDEV RQI
Bio-VD-20	(401-420)	VIRGDEV RQIAPGQTGKIAD
Bio-AT-20	(411-430)	APGQTGKIADYNYKLPDDFT
Bio-YN-20	(421-440)	YNYKLPDDFTGCVIAWNSNN
Bio-GN-20	(431-450)	GCVIAWNSNNLDSKVG GNYN
Bio-LN-20	(441-460)	LDSKVG GNYNYLYR LFRKSN
Bio-YT-20	(451-470)	YLYR LFRKSNLKP FERDIST
Bio-LC-20	(461-480)	LKP FERDISTEIQAGSTPC
Bio-EF-20	(471-490)	EIQAGSTPCNGVEGFNCYF
Bio-NT-20	(481-500)	NGVEGFNCYFPLQSYGFQPT
Bio-PV-20	(491-510)	PLQSYGFQPTNGVGYQPYRV
Bio-NA-20	(501-520)	NGVGYQPYRVV VLSFELLHA
Bio-VV-14	(511-524)	VVLSFELLHAPATV

Extended Data Table 3 | Statistical analysis of cytokine/chemokine levels among severe and critical groups and negative control.

Cytokines	Time point	p-value Negative Control vs Severe	p-value Negative Control vs Critical	p-value Severe vs Critical
GM-CSF (pg/mL)	Initial	0.0282*	0.0209*	0.3022
	Middle	0.0384*	0.0958	0.6078
	Final	0.0002***	0.0847	0.0658
TNF-α (pg/mL)	Initial	0.5501	0.0017**	0.3829
	Middle	0.5808	0.0651	-
	Final	0.2428	0.0001****	0.0042**
TNF-β (pg/mL)	Initial	0.2398	0.3501	-
	Middle	0.2439	0.1003	-
	Final	0.2632	0.7677	-
IFN-γ (pg/mL)	Initial	0.0043**	0.0858	0.7301
	Middle	0.0183*	0.1615	0.6086
	Final	0.1422	0.7925	-
IL-1β (pg/mL)	Initial	0.0004***	0.9697	0.5639
	Middle	0.0032**	0.7656	0.697
	Final	<0.0001****	0.8865	0.4632
IL-2 (pg/mL)	Initial	0.2396	0.289	-
	Middle	0.1133	0.0277*	0.4191
	Final	0.001**	0.4005	0.086
IL-4 (pg/mL)	Initial	0.0921	0.8756	-
	Middle	0.154	0.692	-
	Final	0.0364*	0.9254	-
IL-5 (pg/mL)	Initial	0.0015**	0.0658	0.1313
	Middle	0.0077**	0.1579	0.1916
	Final	0.1669	0.2259	-
IL-6 (pg/mL)	Initial	<0.0001****	0.0007***	0.8631
	Middle	<0.0001****	0.0027**	0.6406
	Final	0.0002***	0.0031**	0.2955
IL-8 (pg/mL)	Initial	<0.0001****	0.0101*	0.7703
	Middle	<0.0001****	<0.0001****	0.445
	Final	0.0021**	<0.0001****	0.6248
IL-9 (pg/mL)	Initial	0.7577	0.3852	-
	Middle	0.6091	0.8354	-
	Final	0.8914	0.5133	-
IL-10 (pg/mL)	Initial	0.2336	0.0672	-
	Middle	0.5711	0.1564	-
	Final	0.8835	0.2994	-
IL-12 (p70) (pg/mL)	Initial	0.4794	0.3895	-
	Middle	0.4177	0.1378	-
	Final	0.0231*	0.267	-
IL-13 (pg/mL)	Initial	0.6309	0.6243	-
	Middle	0.2286	0.238	-
	Final	0.1136	0.2389	-
IL-15 (pg/mL)	Initial	0.0001****	<0.0001****	0.3844
	Middle	0.1305	<0.0001****	0.0241*
	Final	0.1567	0.0007***	0.2552
TGF-β (pg/mL)	Initial	<0.0001****	<0.0001****	0.645
	Middle	0.0009****	0.0015**	0.9841
	Final	0.0087**	<0.0001****	0.0718*
IL-17 a (pg/mL)	Initial	0.3387	0.477	-
	Middle	0.3078	0.2979	-
	Final	0.0918	0.1878	-
IL-17 E/IL-25 (pg/mL)	Initial	0.2233	0.6217	-
	Middle	0.211	0.1854	-
	Final	0.1259	0.7699	-
IL-17 F (pg/mL)	Initial	0.2575	>0.9999	-
	Middle	0.1143	0.4024	-
	Final	0.0368*	0.2454	-
IL-21 (pg/mL)	Initial	0.1691	0.7541	-
	Middle	0.3108	0.1763	-
	Final	0.1689	0.1049	-
IL-22 (pg/mL)	Initial	0.2105	0.7402	-
	Middle	0.2452	0.2491	-
	Final	0.0537	0.2778	-
IL-23 (pg/mL)	Initial	0.0421*	0.7928	-
	Middle	0.278	0.1736	-
	Final	0.0676	0.1738	-
IL-27 (pg/mL)	Initial	0.0059**	<0.0001****	0.6537
	Middle	0.0382*	0.0019**	0.6638
	Final	0.6189	0.0008***	0.0304*
IL-28 a (pg/mL)	Initial	0.2893	0.3545	-
	Middle	0.4155	0.1533	-
	Final	0.3778	0.9847	-
IL-31 (pg/mL)	Initial	0.1947	0.6199	-
	Middle	0.3835	0.153	-
	Final	0.1127	0.501	-
IL-33 (pg/mL)	Initial	0.2134	0.6597	-
	Middle	0.2604	0.1324	-
	Final	0.0752	0.4607	-
MIP3a/CCL20 (pg/mL)	Initial	<0.0001****	0.0059**	0.6168
	Middle	0.0073***	0.0178*	0.3214
	Final	0.0167*	0.0021**	0.9626

* p ≤ 0.05

** p ≤ 0.01

*** p ≤ 0.001

**** p ≤ 0.0001